THE UNIVERSITY OF TEXAS AT AUSTIN

EFFECT OF STEP AND/OR GAP TILE MISALIGNMENT ON SHUTTLE TRANSITION

John J. Bertin and Alan Keisner

Department of Aerospace Engineering and Engineering Mechanics

EFFECT OF STEP AND/OR GAP TILE MISALIGNMENT
ON SHUTTLE TRANSITION

by

John J. Bertin
and
Alan Keisner

AEROSPACE ENGINEERING REPORT 78003

Department of Aerospace Engineering
and Engineering Mechanics

The University of Texas at Austin

June 1978

TABLE OF CONTENTS

Page

INTRODUCTION

In order to predict the convective heat-transfer distribution for the windward surface of the Space Shuttle entry configuration, one must develop engineering correlations for the three-dimensional, compressible boundary-layer. Since the aerodynamic heating rates generated by a turbulent boundary-layer may be several times greater than those for a laminar boundary-layer at the same flight condition, the correlations must include a transition criteria suitable for the complex flow fields. Because the windward surface of the Orbiter is composed of a large number of thermal protection tiles, the transition criteria must include the effect of the distributed roughness arising from the joints and possible tile misalignment.

During tests in which a ring of spherical roughness elements were located in a supersonic flow past a cone, Van Driest and Blumer (ref. 1) observed variations in tne relative roles played by the disturbances in the basic flow field and those resulting from the presence of roughness elements. For some conditions, the disturbances associated with the basic flow field were predominant in establishing transition, whereas for other flows, the roughness elements dominated the transition process.

However, the correlation for the effect of roughness is complicated when other transition-related parameters interact. Morisette (ref. 2) found that although the effective roughness Reynolds number increases significantly in the presence of a favorable pressure gradient near the centerline, much smaller roughness was required to promote transition near the shoulder of an Orbiter configuration, where again there was a favorable pressure gradient (this one associated with cross flow). McCauley et al

1

(ref. 3) found that the spherical roughness elements required to trip the boundary layer on sphere noses were several times larger than the boundary-layer thickness, whereas the trips required for a cone were within the boundary layer. Heat-transfer data (ref. 4) obtained in Tunnel B of the Arnold Engineering Development Center (AEDC) for an 0.04-scale Orbiter indicated that a ring of spherical trips, which were 0.079 cm. (0.031 in.) in diameter and were 0.11L from the nose, caused the transition location to move considerably upstream of the natural transition location (i.e., that for a smooth body). In the same test program (ref. 4), a simulated inter-face gap between two insulation materials, which was 0.102 cm. (0.040 in.) wide by 0.203 cm. (0.080 in.) deep and was located at x = 0.02L, had no measurable effect on boundary-layer transition at α = 40° and $Re_{\infty,L}$ = 8.6 x 10^6. In a series of tests using delta-wing Orbiter models (ref. 5), premature boundary-layer transition was observed on a model having simulated heat-shield panels with raised joints. Slot joints, however, did not cause premature transition of the boundary layer. The former model featured a series of transverse panels 0.635 cm. (0.250 in.) wide separated by a raised retaining strip 0.025 cm. (0.010 in.) wide by 0.0025 cm. (0.001 in.) high. The panels on the model with slotted joints were 0.635 cm. (0.250 in.) square separated by slots 0.020 cm. (0.008 in.) wide by 0.005 cm. (0.002 in.) deep. The Reynolds number ($Re_{\infty,L}$) for these tests ranged from 6.5 x 10^6 to 9.0 x 10^6 using a model 0.403 m. (1.321 ft.) long.

The stability of laminar boundary-layers has been found to be significantly affected by heating or by cooling (usually indicated para-metrically by a temperature ratio, or enthalpy ratio, such as T_w/T_r or T_w/T_e). Lees (ref. 6) found that heat-transfer from the fluid to the wall

stabilized a laminar boundary layer for two-dimensional disturbances and that, if there is a sufficient amount of cooling, the boundary layer on a hydrodynamically, smooth configuration could be completely stabilized. Reshotko (ref. 7) presents data supporting the trend toward complete stabilization. Using the flight data of Rumsey and Lee (ref. 8), Reshotko observed that, for conditions outside the predicted region of complete stabilization, transition did occur (as expected), but at relatively high Reynolds numbers.

However, the unqualified prediction that cooling stabilizes the boundary layer cannot be made since transition reversal has been observed by numerous workers as the model is "cooled" (e.g., refs. 9 and 10). As a result of cooling the boundary layer, there is a relative increase in the magnitude of the disturbance due to a fixed roughness (ref. 11). A further complication is associated with wind tunnel data. Since a low value of T_w/T_r may be obtained either by cooling the wall or by heating the test gas, alternative effects may arise. Using data from a single tunnel, Wagner et al (ref. 12) noted that reducing T_w/T_r by heating the flow significantly decreased $Re_{s,tr}$, possibly because of nonuniform mixing of the supply gas in the stagnation chamber.

Data from an experimental program which was conducted to investigate what effect tile misalignment representative of a reasonable manufacturing tolerance has on heat transfer and transition criteria in the plane-of-symmetry of the Shuttle Orbiter have been analyzed (e.g., ref. 13). The vertical tile misalignment simulated on the 0.0175-scale model was approximately 0.1451 cm. (0.0571 in.) full-scale. Furthermore, the surface temperature for the Tunnel B tests was essentially constant at $0.42T_t$. As

noted in ref. 13, the presence of tile misalignment did not significantly affect the transition locations over the range of test conditions considered. Another test program was conducted in Tunnel F where the windward surface was roughened by a grit blasting technique. The surface temperature for the Tunnel F tests varied from $0.14T_t$ to $0.28T_t$. At the higher Reynolds numbers of the Tunnel F tests, the transition location moved near the nose. The roughness elements became large relative to the boundary layer and became effective as tripping elements. However, there were not sufficient parametric variations to establish suitable correlations.

Analysis of additional data obtained in Tunnel B (AEDC) for a tile-roughened surface (ref. 14) using a 0.0175 scale model of the Space Shuttle Orbiter Configuration for which the first 80% of the windward surface was roughened by a simulated tile misalignment. The experimental heat-transfer data were used to determine the transition locations. Data were obtained for a Mach number of 8 over a Reynolds number range (based on model length) from 1.862×10^6 to 7.091×10^6 with surface temperatures from $0.114T_t$ to $0.435T_t$, with tile-misalignment heights of 0.0025 cm (0.0010 in.) and of 0.0051 cm (0.0020 in.). For these geometries and flow conditions, tile misalignment did not significantly affect the heat-transfer rates in regions where the boundary layer was either laminar or turbulent. This does not exclude the possibility of locally high heating to very small regions (such as tile corners) which could not be measured. Furthermore, when δ^* at $x \gtrsim 0.1L$ was equal to or greater than 0.75k, the experimentally determined transition locations for a tile-roughened cooled model were within 19% of the reference smooth-body transition location at the same freestream conditions. The tile-induced flow perturbations caused significant forward movement of transition only when the theoretical value of δ^* at $x \gtrsim 0.1L$ was less than 0.75k.

The present report presents data correlations relating the location of boundary layer transition on the Shuttle Orbiter to the simulated heat-shield tile misalignments relative to boundary-layer displacement thickness, which incorporates the effects of flow field conditions and surface temperature. The tests were conducted in Tunnel B (AEDC) on a 0.04-scale model of the forward half of the Shuttle Orbiter re-entry configuration. Small clusters of tiles were located on the windward surface near the nose. Each cluster had four moveable tiles while the others were fixed, so that both gap-type misalignments and step-type misalignments could be simulated, as shown in Fig. 1. These clusters of tiles were placed at one of three axial stations, i.e., at $x_{tile} = 0.05L$, at $x_{tile} = 0.111L$, or at $x_{tile} = 0.175L$, as shown in Fig. 2. Data were obtained for a Mach number of 8 over a freestream Reynolds number range (based on the full model length) of from 3.2×10^6 to 14×10^6. The angle of attack was 30° and the surface temperature T_w was $0.43T_t$. The misaligned tiles were -0.0508 cm (-0.020 in.) to 0.0635 cm (0.025 in.) in height with gap-widths from 0.0 cm (0.0 in.) to 0.0508 cm (0.020 in.). Relative transition locations were correlated in terms of the displacement thickness at the tile location, δ^*_{tile}. The results presented in this report illustrate the effect of tile height and gap misalignment on the transition correlations for the various height and gap configurations tested.

EXPERIMENTAL PROGRAM

The objective of this investigation was to determine the effect of tile misalignment, simulating both step-type and gap-type misalignment, on transition locations in the plane of symmetry of the Shuttle Orbiter. Data

were obtained in Tunnel B (Arnold Engineering Development Center), which is a closed circuit hypersonic tunnel with a 50-in. diameter test section providing a Mach number of 8 over a range of pressure levels from 3.45×10^5 N/m² (50 psi) to 6.20×10^6 N/m² (900 psi). The stagnation temperature is sufficient to avoid air liquefaction in the test section and is, therefore, approximately 750°K (1350°R).

Model. - The model is a 0.04-scale configuration of the forward haif of Shuttle Orbiter 140C, as shown in Fig. 2. The model was cast from Lockheed Proprietary Material LH, and consists of a nickel plated copper nose with stainless steel tile sections installed. The reference length, L, is 1.314 m (4.311 ft.) which is based on a full-scale length of 32.8 m (107.8 ft.). The clusters of tiles were located at one of three axial stations shown in Fig. 3. For this report, the configuration will be identified by the axial location of the tile clusters. The configuration notation is as follows:

Configuration Number	Tile Cluster Location
6	x_{tile} = 0.050L
7	x_{tile} = 0.111L
8	x_{tile} = 0.175L

Each cluster had four movable tiles while all others were fixed. The misaligned tiles formed a herringbone pattern (symmetric about the plane of symmetry). The movable tiles could be moved vertically with shims to produce depressions or protuberances. Alternate tiles could be installed to change the gaps between tiles. Stationary tiles were nominally 0.635 cm (0.250 in.) square. Adjustable tiles installed for a 0.0254 cm (0.010 in.) gap were 0.622 cm (0.245 in.) square. Gap changes were made only around the periphery

of adjustable tiles. All other gaps were fixed at 0.0254 cm (0.010 in.).
Simulated heights ranged from -0.0508 cm (-0.020 in.) to 0.0635 cm (0.025 in.)
with gap-width from 0.00 cm (0.00 in.) to 0.0508 cm (0.020 in.).

Chromel-constantan thermocouples were installed in the copper nose
section to monitor the temperature ahead of the tiles during test runs. The
copper nose reduced the wall temperature change ahead of the trip and mini-
mized the boundary layer thickness growth during a run.

The data presented in this report were obtained at a freestream Mach
number of 8 at an angle of attack of 30°, over a Reynolds number range
(based on a full-length model) from 3.2×10^6 to 14×10^6. The surface
temperature T_w was approximately $0.43T_t$. The nominal flow conditions for
the test program are presented in Table 1. For further information concerning
test installation, conditions, and procedures, camera-scanning system, instru-
mentation and precision, and the data reduction system, the reader is referred
to ref. 15 and VKF project V41B-E9A.

THEORETICAL ANALYSIS

The transition locations in this report are presented in terms of the
displacement thickness for theoretical solutions of the nonsimilar laminar
boundary layer. These solutions were obtained using the finite difference
code of ref. 16. This code generates solutions of the laminar boundary layer
f either axisymmetric or two-dimensional configurations with possible ablation
or transpiration cooling (providing that the radius of curvature is large
in comparison to the boundary layer thickness). Solutions for three-dimensional
boundary layers with small cross-flow can be obtained using the axisymmetric
analog (ref. 17) in which an effective radius of curvature is used to describe

streamline divergence. For the present wind-tunnel flow conditions, the thermodynamic properties of the flow were modeled with ideal gas relations (ref. 18). The inviscid flow field and, therefore, the conditions at the edge of the boundary layer were assumed known.

The inviscid flow fields for perfect gas flow past the Shuttle Orbiter at an angle of attack of 30° were supplied by Dr. Goodrich of the NASA-Johnson Space Flight Center (ref. 19). The freestream conditions for which detailed boundary layer solutions were generated are presented in Table 1. The freestream test conditions represented a wide range in Reynolds number. Since the boundary layer thickness at a given station decreases as the Reynolds number increases, the value of the Reynolds number should be considered when determining which streamline is at the edge of the boundary layer. This is important since the entropy of a streamline depends on where that streamline crossed the bow shock wave. Therefore the values of the flow properties at the edge of the boundary layer would depend on the local thickness of the boundary layer. This difference in edge conditions was taken into account in specifying the inviscid boundary conditions for the boundary layer solutions.

Detailed flow fields were supplied by Dr. Goodrich for only four values of the Reynolds number. Referring to Table 1, they are: $Re_{\infty,L} = 2.2 \times 10^6$ (designated W31), 4.3×10^6 (designated W32), 6.5×10^6 (designated W33), and 10.8×10^6 (designated W34). Hence, for all other freestream Reynolds numbers studied, the required boundary layer parameters were determined using correlations for the local Reynolds number as a function of the wetted distance from the stagnation points (Fig. 4) and for the displacement thickness for the detailed boundary layer solutions (Fig. 5). The equation used to calculate the displacement thickness δ^* is that for a compressible flow:

$$\delta^* = \int_0^\delta (1 - \frac{\rho u}{\rho_e u_e})dy$$

For a specified distance from the stagnation point the local Reynolds number can be determined using Fig. 4. Once the local Reynolds number is known, the displacement thickness can be found using Fig. 5. The transition correlation parameters for all freestream Reynolds numbers other than those for the supplied detailed boundary layer solutions were computed using this double interpolation routine.

DISCUSSION OF RESULTS

The heat-transfer distributions obtained in the experimental program were used to determine the transition location. The transition location for a given flow-condition/model-configuration was defined to be that point at which the experimentally-determined heat-transfer rate first departed from the laminar distribution. The transition locations thus determined are presented in Table 2. For many of the test conditions, boundary-layer transition was fixed at the tile cluster. Tile misalignment was simulated by combinations of step and/or gap mismatch. Step heights (measured from the smooth-body wall) ranged from -0.0508 cm (-0.020 in.) to 0.0635 cm (0.025 in.) with gap widths from 010 cm (0.0 in.) to 0.0508 cm (0.020 in.). For the three configuration groupings studied, the tiles were located at: $x_{tile} = 0.050L$, designated C6; $x_{tile} = 0.111L$, designated C7; or $x_{tile} = 0.175L$, designated C8.

The experimentally-determined transition locations are presented in Figs. 6 through 10 as a function of Re_{ns}, the Reynolds number based on conditions behind a normal shock,

$$Re_{ns} = \frac{\rho_{ns} U_{ns} r_{ref}}{\mu_{ns}}$$

For these tests the local Reynolds number Re_x at a given location is approximately proportional to the Reynolds number behind the normal shock wave Re_{ns} over the range of freestream Mach numbers and freestream Reynolds numbers $Re_{\infty,L}$ considered. Smooth-body transition locations are also presented in Figs. 6 through 10. The smooth-body transition locations are given by

$$(x_{tr}/L)_{corr} = 4.3131 - 0.98 \log_{10} Re_{ns} \tag{1}$$

which was developed in ref. 14. The transition locations calculated using this correlation are summarized in Table 1.

When comparing the "measured" tile-perturbed transition locations with the "calculated" smooth-body transition locations, the reader should keep in mind that the correlation represented by equation (1) was developed using data for a significantly different, full-length model in the same wind tunnel. It might also be noted that a smooth-body correlation presented in Fig. 27 of ref. 15 gave transition locations significantly different than those of equation (1). However, the smooth-body transition locations calculated using a correlation developed independently by Dr. Goodrich gave essentially the same values as equation (1).

Figure 6 illustrates the movement of transition locations as a function of the Reynolds number behind the normal shock wave for a gap width of $w = 0.0254$ cm (0.010 in.) and a tile height difference of $k = 0.0381$ cm (0.015 in.). For Reynolds numbers equal to or greater than $Re_{ns} = 6.5 \times 10^3$, transition appears to be fixed for configurations C6 and C7. The term "fixed" implies that transition occurs at the tile location itself. A slight knee appears in the

curve for configuration C8, indicating that transition for this configuration was not fixed at the tiles until a Re_{ns} of 8.3×10^3 was reached. This may be due to the fact that, for a given Reynolds number, the boundary layer was thickest at the configuration 8 tiles due to their relative downstream location. Note that the Reynolds number-dependence of the nonfixed transition locations for each configuration approximated that of the smooth-body in sequential order with transition occurring nearest the nose for C6, then for C7 and ultimately for C8. This might be expected from the location of the tile clusters relative to the nose. The transition location moves steadily forward toward the tile location for increasing Reynolds numbers until it occurs at the tiles. The point designated "wholly laminar" for C8 at $Re_{ns} = 4.3 \times 10^3$ indicates that transition did not occur for this condition. Since only the first 50% of the vehicle was simulated, this point may in reality represent a transition location anywhere from $x_{tr} = 0.50L$ to the smooth-body correlation at $x_{tr} = 0.75L$ (as indicated by the arrow).

The effect of gap width on the transition location is indicated in Fig. 7. Data are presented for widths of w = 0.0 cm (0.0 in.), w = 0.0254 cm (0.010 in.) and w = 0.0508 cm (0.020 in.), all for a tile height misalignment of k = 0.0254 cm (0.010 in.). Transition fixing was a function of the tile location. Transition became fixed at lower Reynolds numbers as the location of the tile clusters was placed nearer the nose. This is illustrated in the data of Figs. 7b and 7c. For the largest gap width, w = 0.0508 cm (0.020 in.), transition for C6 was fixed for $Re_{ns} \geq 6.5 \times 10^3$, while for C7 it was fixed for $Re_{ns} \geq 7.5 \times 10^3$. As the gap width increased, transition fixing occurred at lower values of the Reynolds number for each configuration. This can be seen in Fig. 7, since transition fixing for C7 occurs at approximately $Re_{ns} = 8.5 \times 10^3$ for a gap

Of 0.0 cm (0.0 in.)(see Fig. 7a), at $Re_{ns} = 8 \times 10^3$ for a gap of 0.0254 cm (0.010 in.)(see Fig. 7b), and at $Re_{ns} = 7.5 \times 10^3$ for a gap of 0.0508 cm (0.020 in.)(see Fig. 7c). As noted when discussing the data presented in Fig. 6, below these critical values of Re_{ns}, the transition location moves forward to the trip as the Reynolds number increases. Again, as the gap width was increased, the initial trip transition Reynolds number Re_{ns} decreased for each corresponding configuration in order of the location of the tile clusters from the nose. An interesting result, presented in Fig. 7b, reveals that for a slight increase in local Reynolds number transition location moves markedly forward to the trip for C7, whereas that for C8 follows the correlation for the smooth-body correlation. The reason that the transition location occurs relatively further downstream for the C7 configuration is not known at present. However, the tile patterns were changed using inserts and spacing shims, and the C7 tests were conducted relatively early in the experimental program. It is possible, therefore, that surface roughness (excluding the tiles themselves) was different, i.e., the alignment of the configuration may have been affected. For a given local Reynolds number Re_x (which is approximately proportional to the Reynolds number behind a normal shock wave, Re_{ns}), the displacement thickness at the tile δ^*_{tile} decreases as tile grouping moves forward. The relatively downstream transition location measured at $Re_{ns} = 12.9 \times 10^3$ for the C7 configuration with w = 0.0 cm (0.0 in.) is believed to be due to experimental error.

The transition location is presented in Fig. 8 as a function of the local Reynolds number downstream of the normal shock wave for C7 ($x_{tile} = 0.111L$) with a roughness height misalignment at k = 0.0254 cm (0.010 in.) for various gap widths. The larger the gap, the greater the possibility that transition will advance to the trip for a given Reynolds number. Thus, as

illustrated by these data, a gap can be an effective device in promoting transition of the boundary layer and, consequently, in effecting local heating rates. Again, there are some unexplained anomalies in the data, e.g., the relatively late transition at Re_{ns} = 12.9 × 10³ for the configuration with no gap.

The transition location is presented as a function of Reynolds number in Fig. 9 for C8 (x_{tile} = 0.175L) for a step height of k = 0.0381 cm (0.015 in.). Again, the transition location is affected by various gap widths. However, for these tests, a surprising trend is evident: transition occurred nearer the nose for gaps of decreasing width. This trend is opposite to that previously noted for C7 in Fig. 8. A pronounced anomaly in this surprising trend is evident for the widest gap w = 0.0508 cm (0.020 in.). The reason for the occurrence of a relatively stable boundary layer for this width is unknown. Again, these data were obtained in runs which were made early in the test program and shortly after those for the relatively stable, un-explained data for configuration C7 (Fig. 7b). Since this occurred in approxi-mately the same portion of the program, the possibility that the model was slightly different for these cases must be considered. As before, the transition location of the "wholly laminar" point may vary between 0.5L and the smooth-body location.

The effect of gap-only roughness where w = 0.0254 cm (0.010 in.) with k = 0.0 cm (0.0 in.) on the relationship between transition location and Reynolds number for this condition is illustrated in Fig. 10. Variation in transition location for the Reynolds numbers tested for C7 is minor, e.g., x_{tr} varies from 0.35L to 0.40L. It is more pronounced for the C6 configuration, for which the tiles are nearer the nose. Thus, with no step-type misalignment,

i.e., $k = 0.0$ cm (0.0 in.), the presence of a gap promoted transition but in no case did transition proceed upstream to the tile location (Fig. 3), i.e., transition was not fixed. Nevertheless, gap-only roughness can be an important factor in determining the transition location, especially near the nose where the natural boundary layer is thinnest.

The Relative Transition Locations

As evident in the data presented in Figs. 6 through 10, transition was fixed at the tile clusters for many of the test conditions. Data from these runs provide relatively little information which can be used to develop correlations defining the effect of tile misalignment on the transition location. Therefore, data for those tests where transition occurred at the tile itself, i.e., where the transition process was "instantaneous," are not presented in Figs. 11 through 17.

The relative transition location is defined as:

$$\xi = x_{tr}/x_{tr,0} \tag{2}$$

which is the ratio of the perturbed transition location to the smooth-body transition location. The relative transition location is presented in Fig. 11 as a function of k, the tile misalignment height. Note that, since the tile clusters are located at 0.175L for the C8 configuration and at 0.050L for the C6 configuration, the tile-perturbed transition locations were further downstream for the C8 configuration and, therefore, nearer the natural (smooth-

body) transition location. As a result, the values of ξ for a given tile step height are usually larger for C8. Furthermore, at the relatively high freestream Reynolds numbers, e.g., 10.8×10^6 and 12.9×10^6, where natural transition occurs relatively near the nose, the presence of a tile cluster at $x_{tile} = 0.175\ell$ (configuration C8) moved transition only slightly upstream. Thus, the values of ξ for these tests were relatively high. Note that the depressed tiles (i.e., a negative misalignment height) were effective in promoting transition, although not quite as effective as a protuberance.

The transition locations from the present tests are compared with the data from ref. 14 as a function of tile height mismatch and displacement thickness for configurations with no gap width, w = 0.0 cm (0.0 in.). As noted in the Introduction, the data from ref. 14 were obtained in Tunnel B (AEDC) using a 0.0175-scale model of the Shuttle Orbiter for which the first 80% of the windward surface was roughened by simulated tile misalignment. As was the case for the present data, the experimental heat-transfer data, which were used to determine transition locations, were obtained for a Mach number of 8 over a Reynolds number range (based on model length) from 1.8×10^6 to 7.1×10^6 for surface wall temperatures from $0.114T_t$ to $0.435T_t$. Since the tiles were distributed over the surface of the ref. 14 model, the displacement thickness δ^* was calculated at x = 0.1L. For the present tests, the displacement thickness was evaluated at the tile clusters. For the relatively high values of the ratio k/δ^*_{tile}, the present data agree well with previous findings. However, for a gap width of 0.0 cm (0.0 in.) no data were obtained in the present program for which tiles did not affect the transition location.

The relative transition locations are presented in Fig. 13 as a function both of the gap width and of the step height. With limited exceptions, the

ᵗᵉⁿᵈ for all three configurations is that ξ decreases as one moves from the origin. I.e., various combinations of gap width and step height promoted transition with the larger gap and higher steps providing the most pronounced effect. For the C8 configuration, however, many local variations are evident for combinations of misalignments. Such specific or local deviations from the general trends are attributed to experimental uncertainty.

The data of Fig. 12 are presented again in Fig. 14a, showing the relative transition location as a function of the displacement thickness and roughness height at the trip for a gap width w = 0.0 cm (0.0 in.). Generally, transition moved upstream depending on configuration locations, as can be expected. Increasing Reynolds numbers had a slight effect in the relative transition location for a given tile height misalignment. For Figs 14b and 14c, both tile gap and height mismatch are presented. Values for the transition parameter ξ are low even when the ratio δ^*_{tile}/k exceeds unity. In fact, $0.4 < \xi < 0.6$ for the infinite magnitude of the ratio δ^*_{tile}/k, which obviously describes the effect of the gap-only misalignment. "Wholly laminar" points were arbitrarily assigned for a ξ value of unity. It is possible that had a full-length model been tested, the tile misalignments would have caused transition to occur upstream of the natural transition location. As has already been discussed, the values of ξ were usually the smallest when the misaligned tiles were nearest the nose. Since the tiles significantly perturb the flow, one would expect the transition location to move upstream as the perturbation mechanism is moved upstream.

One should not oversimplify the problem and conclude that moving the tile perturbation upstream will always move transition proportionally upstream. Moving a given tile-misalignment geometry (i.e., specific values for gap width

and step height) upstream causes the value of δ^*_{tile}/k to decrease for a given flow condition, since the boundary layer is thinner. However, for a given flow condition, the local Reynolds number is also smaller nearer the nose. It is possible that, if the local Reynolds number were small enough, a tile-induced perturbation would not be amplified to cause premature transition. Although complete damping of the tile-induced perturbations was not observed, the distance from the tile cluster to the transition location usually increased when the cluster was moved nearer the nose. This interaction between the transition-related parameters is indicated in Fig. 15, where the data are presented as a function of $(x_{tr} - x_{tile})/L$. Since one would expect transition to move forward as the tiles were moved forward, this parameter was therefore considered as a possible indicator of whether or not the distance from the tile to the transition location was approximately the same for a given roughness. An apparent trend for this parameter with gap width w = 0.0254 cm (0.010 in.) is that the configuration with the tile cluster furthest downstream, C8, caused the shortest run to achieve transition, since it occurred near or at the trip itself. This might be expected for the configurations tested. For C7 and for C6, transition occurred further downstream from the tile grouping. As roughness height increases the location of transition from the tile cluster decreases, especially for high freestream Reynolds numbers, where the tile location was very near that for transition. For a few points $(x_{tr} - x_{tile})/L$ is less than zero, indicating tile-induced transition occurred upstream of the trip. Since this is not possible for these test conditions, the negative values are attributed to errors in defining the transition location. Again for cavities, increasing the freestream Reynolds number

decreased the relative distance between transition and tile location. Inconsistent patterns are obtained for various width and height misalignments. Hence, no freestream Reynolds number correlation appears possible at present with this data.

Another attempt to isolate the relevance of distance from the tile to transition is presented in Fig. 16 where relative transition location is based on the smooth-body natural transition location $x_{tr,0}$. This has an effect of grouping the data by order of configuration from the nose from left to right as a function of the ratio δ^*_{tile}/k.

To account for the effects both of gap width and of step height, the data were correlated using a "Pythagorean" approach, as shown in Fig. 17. Since the gap width and the tile height mismatch clearly play a joint role in promoting transition, this method was chosen to indicate the combined effect while avoiding the situation where δ^*_{tile}/k becomes infinite because $k = 0.0$ cm (0.0 in.). The effective misalignment parameter was specified as k_{eff}, where $k_{ei} = \sqrt{k^2 + w^2}$. This parameter is more representative of the effect of combined width and height misalignment. However, it is not a completely satisfactory parameter because, as has been noted previously, the gaps are not equally effective as the heights in promoting transition.

CONCLUDING REMARKS

The effect of tile misalignment on the boundary layer transition location has been studied. Transition data were obtained for a variety of misalignment height and gap width in the tile clusters, where the clusters were located either at 0.050L, at 0.111L, or at 0.175L. For the configurations tested, the tile roughness was so severe that transition occurred at the tile

configurations themselves, i.e., it was fixed, for many of the runs tested. However, based on the data available, the following conclusions are reached:

1. Gaps, even by themselves, promote transition. However, a gap of a given width was not as effective as a step of equal height.

2. Tiles which are depressed (a negative misalignment height) were not quite as effective in promoting transition as tiles which protrude above the adjacent tiles in the configuration (a positive misalignment height).

3. At the highest Reynolds numbers the relative transition locations (ξ) are relatively large since the natural transition locations are not very far downstream of the location of the tile clusters. Therefore, only a relatively small forward movement of transition due to roughness would be possible.

NOMENCLATURE

k	height of the misaligned tiles
L	axial model length, 1.314 m
M	Mach number
r_{ref}	radius of the reference sphere, 0.0122 m
Re_{ns}	Reynolds number based on flow conditions behind a normal shock
Re_x	Reynolds number based on local flow properties integrated along the wetted distance along a streamline
$Re_{\infty,L}$	Reynolds number based on freestream flow properties and the model length
T	temperature
T_r	recovery temperature
u	x-component of the velocity
w	gap width of the misaligned tiles
x	axial coordinate
y	coordinate measured normal to the model surface
δ^*	displacement thickness
μ	viscosity
ρ	density
ξ	relative transition location defined in equation 2

Subscripts

e	evaluated at the edge of the boundary layer
ns	evaluated downstream of a normal shock wave
$tile$	evaluated at the location of the tile cluster
tr	evaluated at the transition location
$tr,0$	evaluated at the transition location for the smooth model, also $(x_{tr})_{corr}$
w	evaluated at the wall
∞	evaluated at the freestream conditions

REFERENCES

1. van Driest, E.R., and Blumer, C.B., "Boundary-Layer Transition at Supersonic Speeds - Three-Dimensional Roughness Effects (Spheres)", Journal of the Aerospace Sciences, Aug. 1962, Vol. 29, No. 8, pp. 909-916.

2. Morrisette, E.L., "Roughness Induced Transition Criteria for Space Shuttle-Type Vehicles", Journal of Spacecraft and Rockets, Feb. 1976, Vol. 13, No. 2, pp. 118-120.

3. McCauley, W.D., Saydah, A.R., and Bueche, J.F., "Effect of Spherical Roughness on Hypersonic Boundary-Layer Transition", AIAA Journal, Dec. 1966, Vol. 4, No. 12, pp. 2142-2148.

4. Carver, D.G., "Heat-Transfer Tests on the Rockwell International Space Shuttle Orbiter with Boundary-Layer Trips (OH-54)", AEDC-TR-76-28, May 1976.

5. Seegmiller, H.L., "Effects of Roughness on Heating and Boundary Layer Transition, Part I - Effects of Simulated Panel Joints on Boundary-Layer Transition", Space Shuttle Aerothermodynamics Technology Conference, Volume II-Heating, NASA TM X-2507, February 1972.

6. Lees, L., "The Stability of the Laminar Boundary Layer in a Compressible Fluid", NACA Report No. 876, 1947.

7. Reshotko, E., "Transition Reversal and Tollmien-Schlichting Instability", Physics of Fluids, March 1963, Vol. 6, No. 3, pp. 335-342.

8. Rumsey, C.B. and Lee, D.B., "Measurements of Aerodynamic Heat Transfer and Boundary-Layer Transition on a 10° Cone in Free Flight at Supersonic Mach Numbers Up to 5.9", NASA TND-745, May 1961.

9. Diaconis, N.S., Jack, J.R. and Wisniewski, R.J., "Boundary-Layer Transition at Mach 3.12 as Affected by Cooling and Nose Blunting", NACA TN 3928, January 1957.

10. Richards, B.E. and Stollery, J.L., "Further Experiments on Transition Reversal at Hypersonic Speeds", AIAA Journal, December 1966, Vol. 4, No. 12, pp. 2224-2226.

11. Potter, J.L. and Whitfield, J.D., "The Relation Between Temperature and the Effect of Roughness on Boundary-Layer Transition", Journal of the Aerospace Sciences, August 1961, Vol. 28, No. 8, pp. 663-664.

12. Wagner, R.D., Maddalon, D.V., Weinstein, L.M., and Henderson, A. Jr., "Influence of Measured Free-Stream Disturbances on Hypersonic Boundary-Layer Transition", AIAA Paper 69-704, presented at 2nd Fluid and Plasma Dynamics Conference, San Francisco, June 1969.

13. Bertin, J.J., Stalmach, D.D., Idar, E.S., Conley, D.B., and Goodrich, W.D., "Hypersonic Heat-Transfer and Transition Correlations for a Roughened Shuttle Orbiter," presented at the 13th Annual Meeting of the Society of the Engineering Sciences, Hampton, Virginia, November 1976.

14. Bertin, J.J., Idar, E.S., and Galanski, S.R., "Effects of Surface Cooling and of Roughness on the Heating (Including Transition) to the Windward Plane-of-Symmetry of the Shuttle Orbiter," Aerospace Engineering Report 77002, April 1977, University of Texas at Austin.

15. Hube, F.K., "Simulated Thermal Protection Tile Roughness Effects on the Windward Surface Heat Transfer on the Rockwell International Space Shuttle Orbiter," AEDC-TR-76-98, January 1977.

16. Stalmach, D.D. and Bertin, J.J., "Analysis of a Nonsimilar Laminar Boundary-Layer," Aerospace Engineering Report 78001, February 1978, University of Texas at Austin.

17. Cooke, J.C., "An Axially Symmetric Analogue for General Three-Dimensional Boundary Layers," British Aeronautical Research Council, R&M 3200, 1961.

18. van Wylen, G.J., Thermodynamics, John Wiley & Sons, Ltd., New York, 1959.

19. Goodrich, W.D., private communication, January 1978.

Table 1. - Nominal Flow Conditions

P_{t2} Stagnation Pressure (psfa)	T_t Stagnation Temperature (°R)	$Re_{\infty,L}$ Free Stream Reynolds Number	Re_{ns} Reynolds Number Behind Normal Shock	$(x_{tr}/L)_{corr}$ Transition Correlation for smooth model, Equation (1)	Detailed Computer Solution for the Laminar Boundary Layer
-	-	2.155×10^6	-	-	yes (W31)
151.7	1275	3.156×10^6	3,222	0.855	no
210.2	1271	4.354×10^6	4,453	0.716	yes (W32)
263.8	1288	5.367×10^6	5,473	0.628	no
323.7	1289	6.553×10^6	6,671	0.543	yes (W33)
374.2	1289	7.557×10^6	7,674	0.483	no
422.9	1294	8.458×10^6	8,581	0.435	no
492.1	1308	9.687×10^6	9,864	0.376	no
556.2	1320	10.760×10^6	10,968	0.330	yes (W34)
612.2	1329	11.726×10^6	11,981	0.293	no
670.2	1331	12.812×10^6	13,100	0.254	no

Table 2. - The transition locations (x_{tr}/L) for the 0.04-scale Orbiter model with misaligned tile clusters.

x_{tr}/L for:

Config	Gap w (cm)	Height k (cm)	Nominal freestream Reynolds number $Re_{\infty,L}$ ($\times 10^{-6}$)							
			3.156	4.354	5.367	6.553	7.557	8.458	9.687	10.760
C6	0.0000	0.0254	-	-	-	-	0.175	fixed	fixed	fixed
C6	0.0254	0.0000	-	-	-	0.251 to 0.294	-	0.188	-	-
C6	0.0254	0.0127	-	-	-	0.200	C.100 to 0.127	fixed	fixed	fixed
C6	0.0254	0.0254	-	0.235	0.192 to 0.172	fixed	fixed	fixed	fixed	fixed
C6	0.0254	0.0381	-	0.175	0.125	fixed	fixed	fixed	fixed	fixed
C6	0.0508	0.0254	-	0.210	0.138	fixed	fixed	fixed	fixed	fixed
C7	0.0000	0.0254	-	-	-	-	0.184	fixed	fixed	fixed
C7	0.0254	-0.0508	-	-	-	0.250 to 0.280	0.193 to 0.197	fixed	fixed	fixed
C7	0.0254	0.0000	-	0.300	-	0.291	-	0.258	-	-
C7	0.0254	0.0254	-	-	wholly laminar	0.337	fixed	fixed	fixed	-
C7	0.0254	0.0381	-	0.250	0.175	fixed	fixed	fixed	fixed	-

Table 2. - Concluded.

| | | | x_{tr}/L for: | | | | | | | |
| | | | Nominal freestream Reynolds number $Re_{\infty,L}$ ($\times10^{-6}$) | | | | | | | |
Config	Gap w (cm)	Height k (cm)	3.156	4.354	5.367	6.553	7.557	8.458	9.687	10.760
C7	0.0254	0.0508	0.248	0.200	fixed	fixed	fixed	fixed	-	-
C7	0.0508	0.0254	-	-	0.232	0.15	fixed	fixed	fixed	fixed
C8	0.0000	0.0381	-	0.286	0.183	fixed	fixed	fixed	fixed	fixed
C8	0.0254	- 0.0508	-	-	-	-	-	0.200	fixed	fixed
C8	0.0254	0.0254	-	-	0.315 to 0.342	0.285	0.215	fixed	fixed	fixed
C8	0.0254	0.0381	-	wholly laminar	0.273	0.192	0.192	fixed	fixed	fixed
C8	0.0254	0.0635	0.20	fixed	fixed	fixed	0.188	0.175	0.178	0.185
C8	0.0508	0.0381	-	0.313	0.400	0.340	0.190	0.178	0.181	0.180 to 0.191
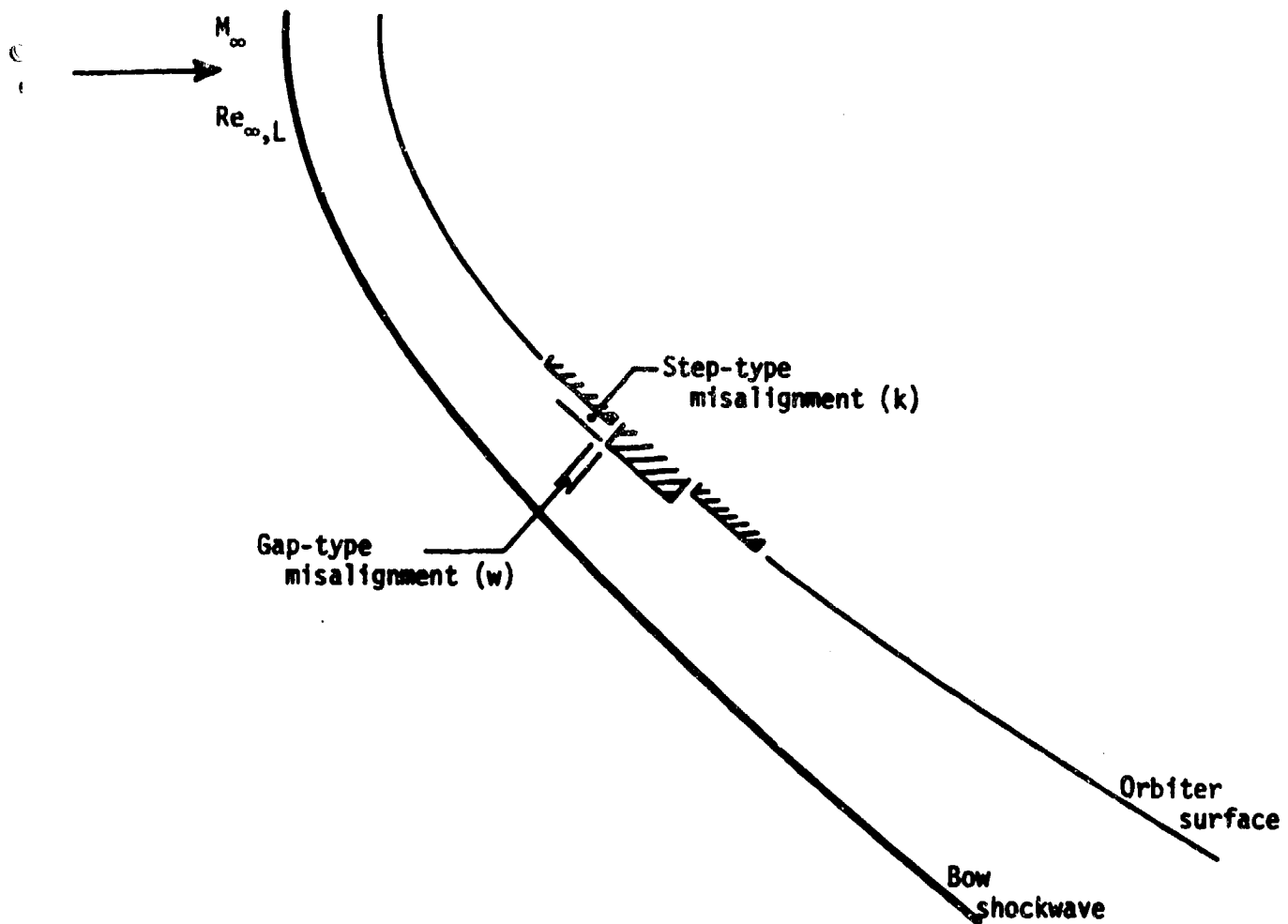
Figure 1. - A sketch of the misalignment for the Shuttle Orbiter TPS
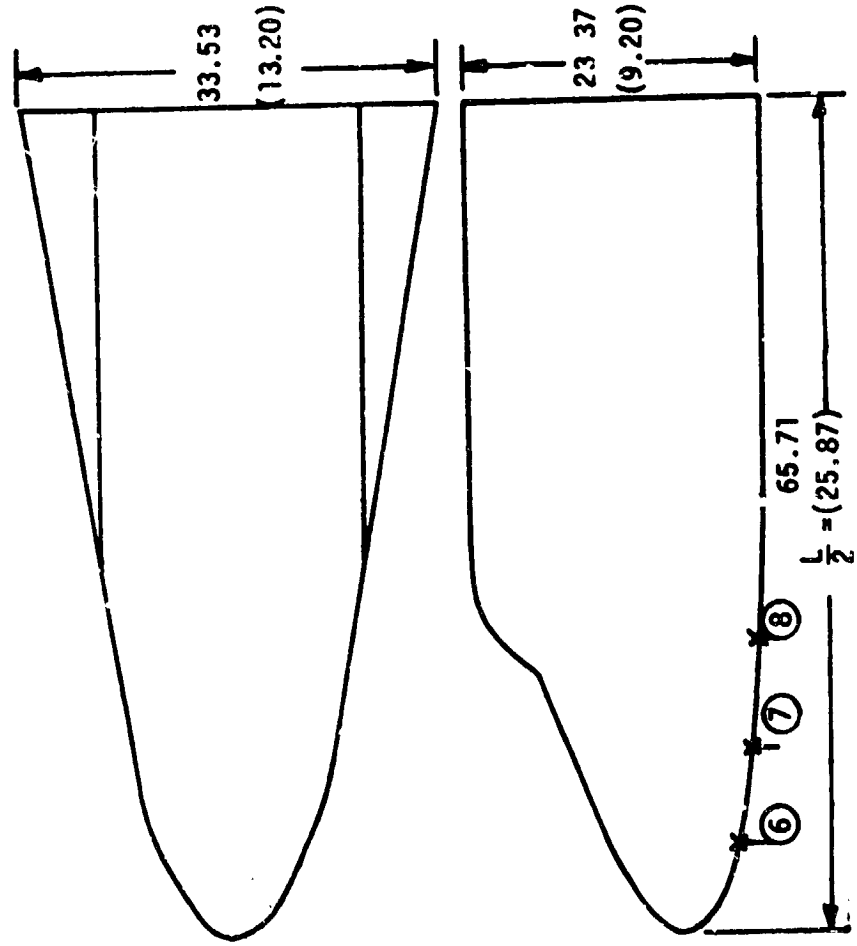
Note all dimensions in centimeters
(inches)
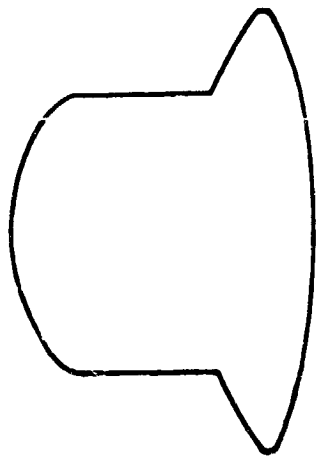
* Tile locations
◯ Configuration no.

33.53
(13.20)

23 37
(9.20)

65.71
$\frac{L}{2}$ = (25.87)

⑧

⑦

⑥

Figure 2. - A sketch of the 0.04-scale, half-length Shuttle model illustrating the three stations at which the tile patterns were located.
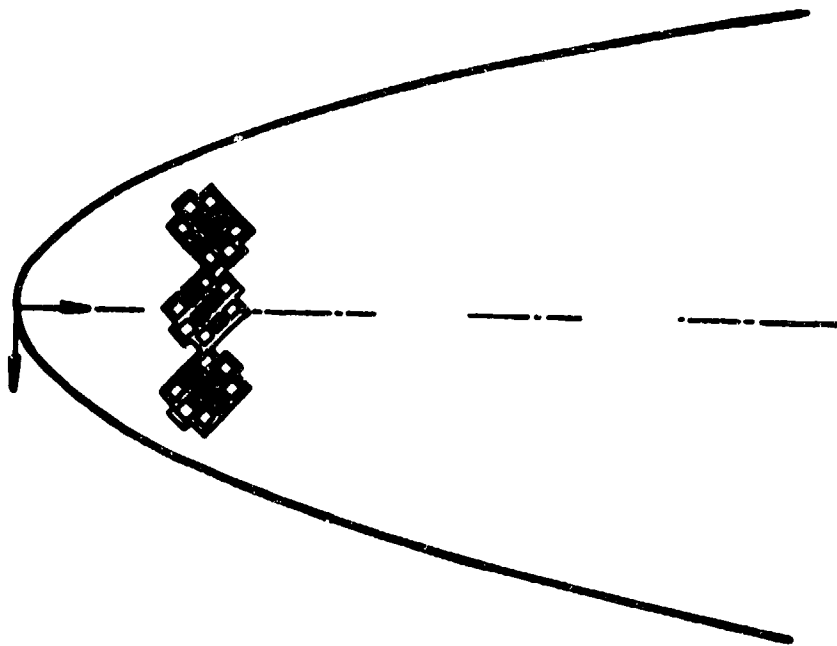
(a) C6, $\dfrac{x_{tile}}{L}$ = 0.050

Figure 3. - Sketches of the tile patterns
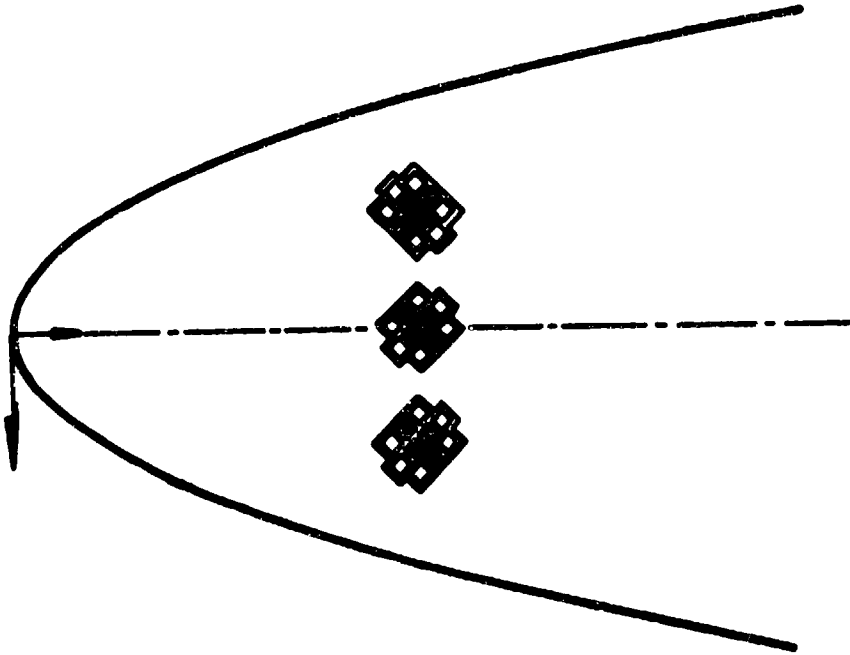
(b) C7, $\dfrac{x_{tile}}{L} = 0.111$

Figure 3.- Continued.
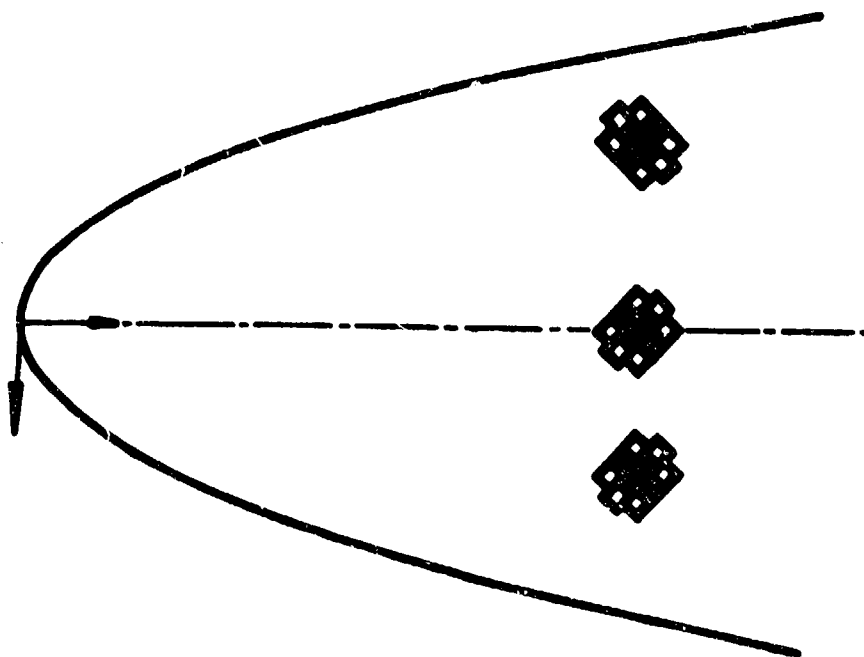
(c) C8, $\frac{x_{tile}}{L}$ = 0.175

Figure 3. - Concluded.
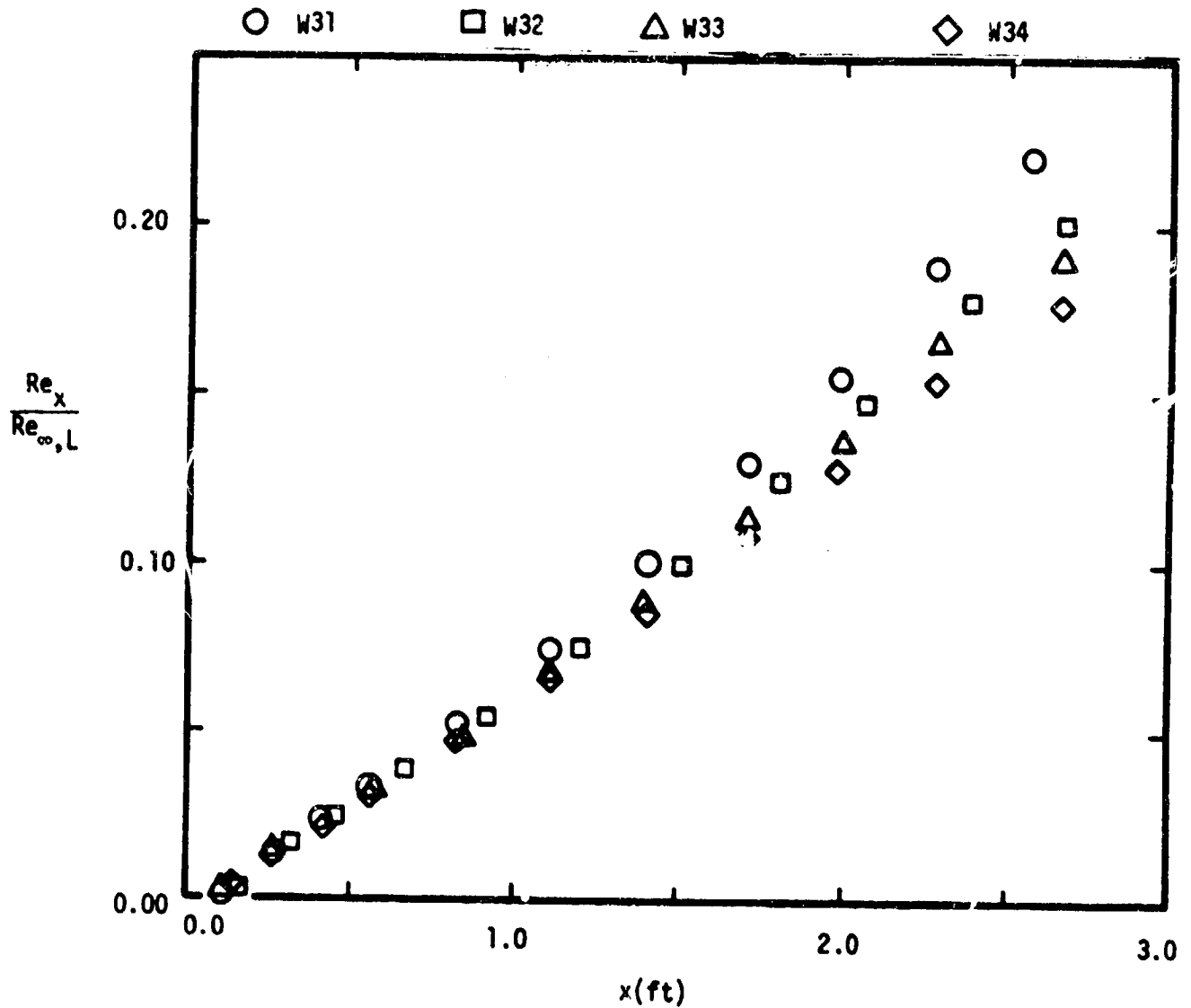
Figure 4. – The local Reynolds number as a function of the wetted distance from the stagnation point for the detailed boundary-layer solutions
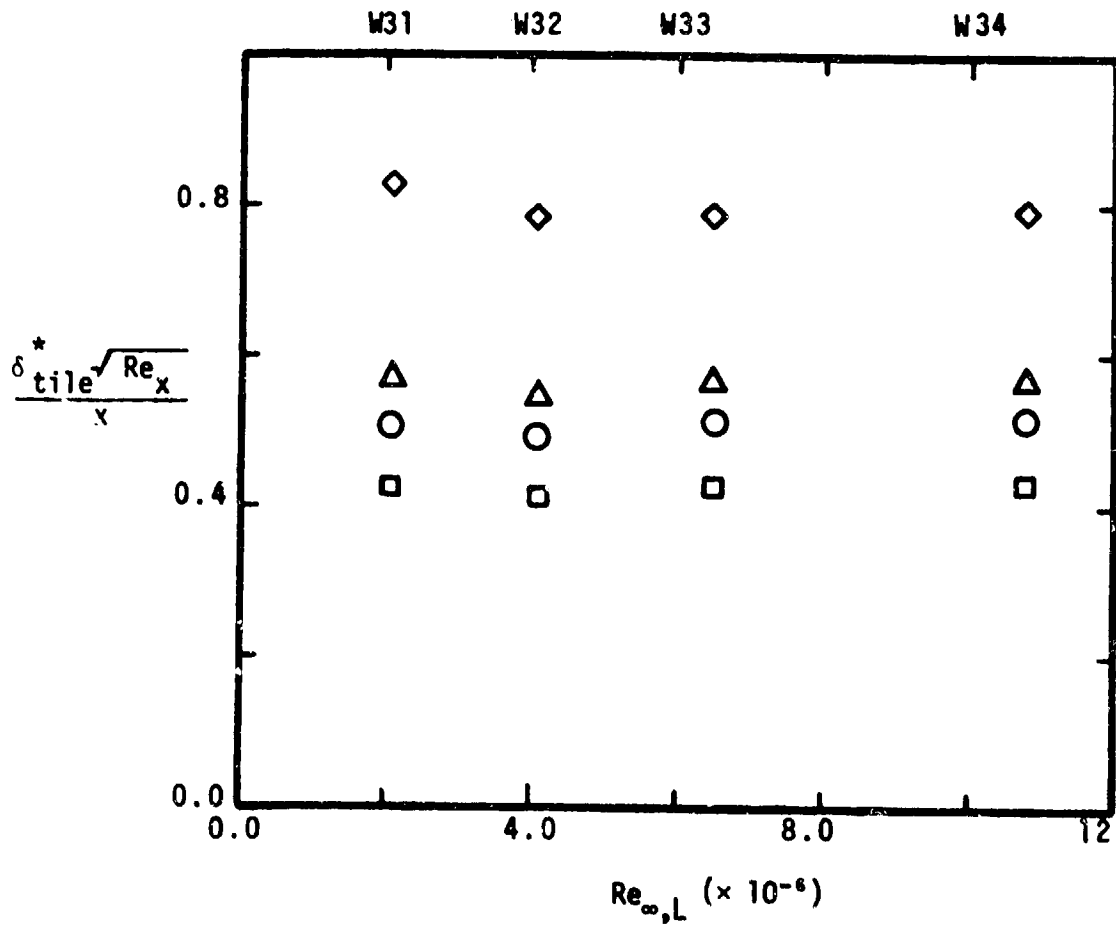
Figure 5. - The displacement thickness correlation for the detailed boundary layer solutions
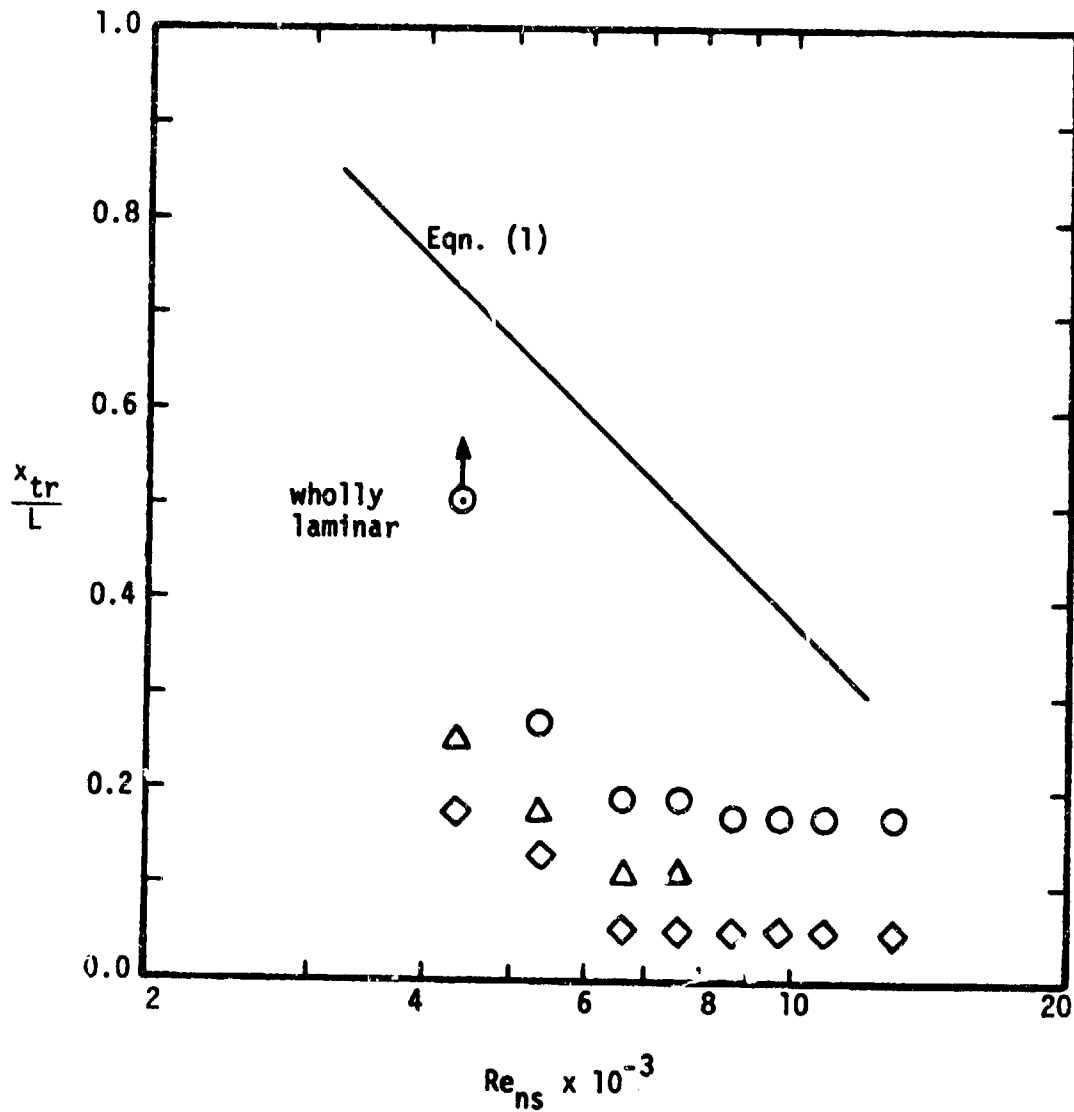
Figure 6. - The transition location as a function of Re_{ns} for
$w = 0.0254$ cm (0.010 in) and $k = 0.0381$ cm (0.015 in)
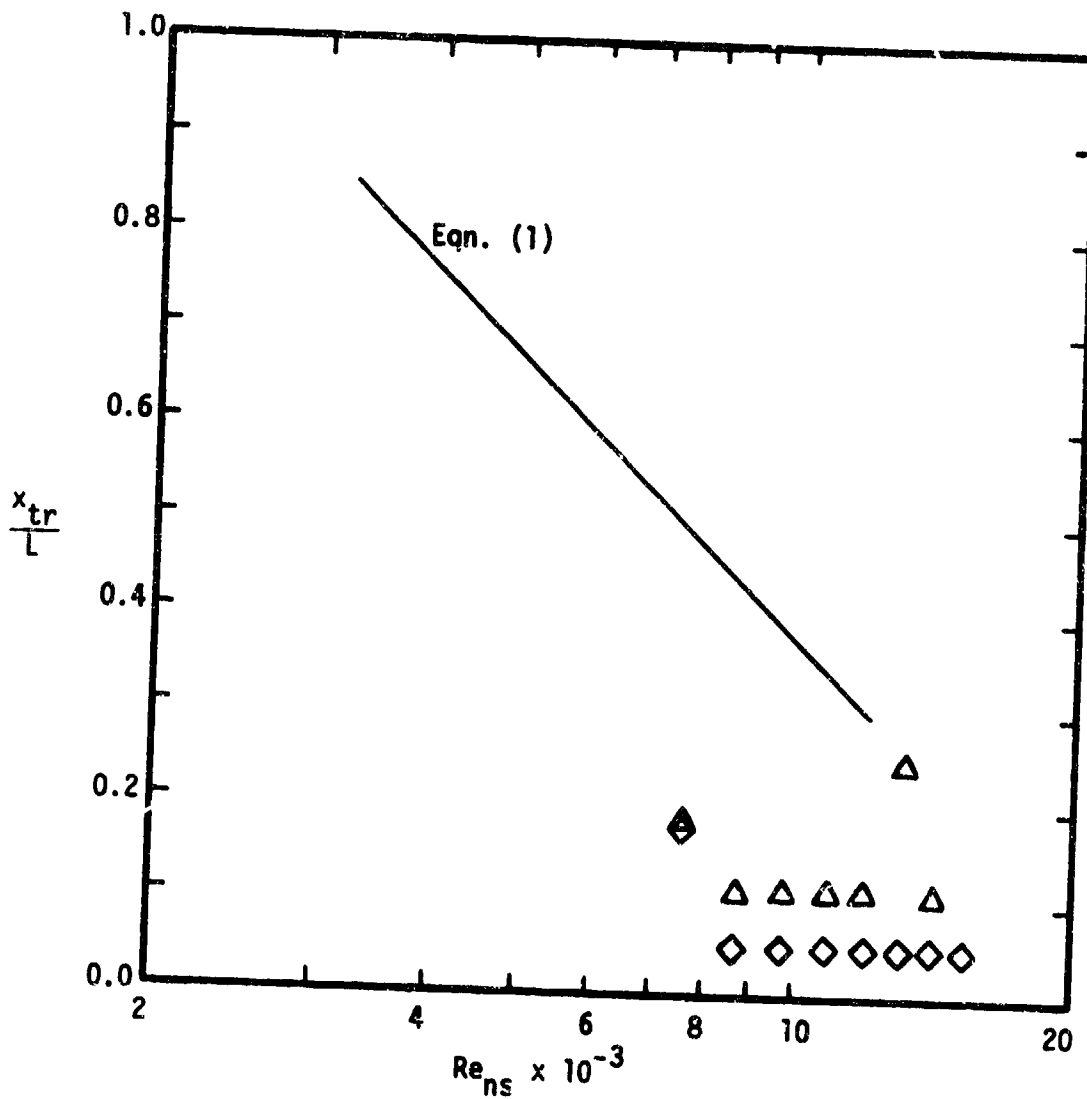
(a) w = 0.0 cm (0.000 in.)

Figure 7. - The transition location as a function of Re_{ns} for various gap dimensions, k = 0.0254 cm (0.010 in.)
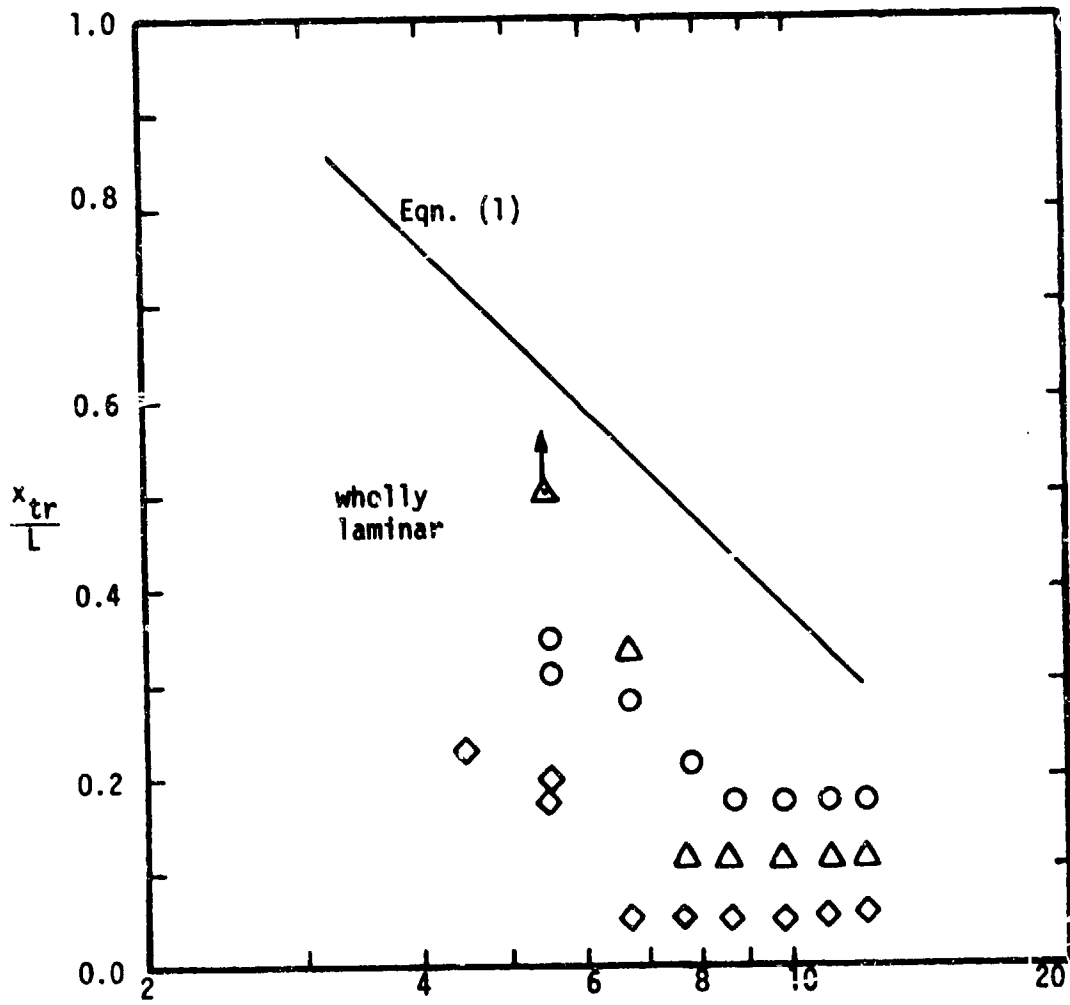
Figure 7. - Continued.

◇ C6

△ C7

$\dfrac{x_{tr}}{L}$

Eqn. (1)

$Re_{ns} \times 10^{-3}$
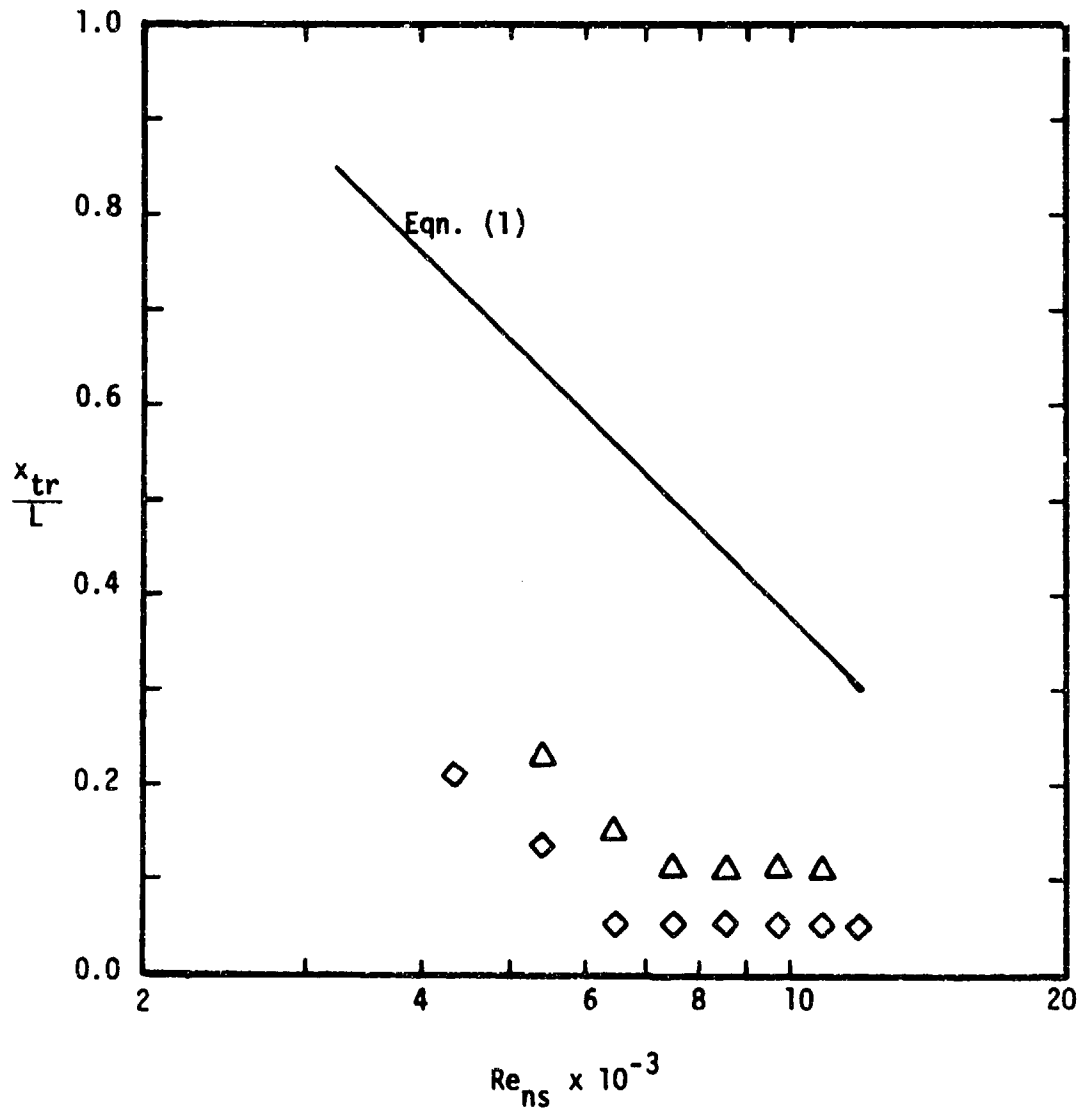
(c) w = 0.0508 cm (0.020 in.)

Figure 7. - Concluded.
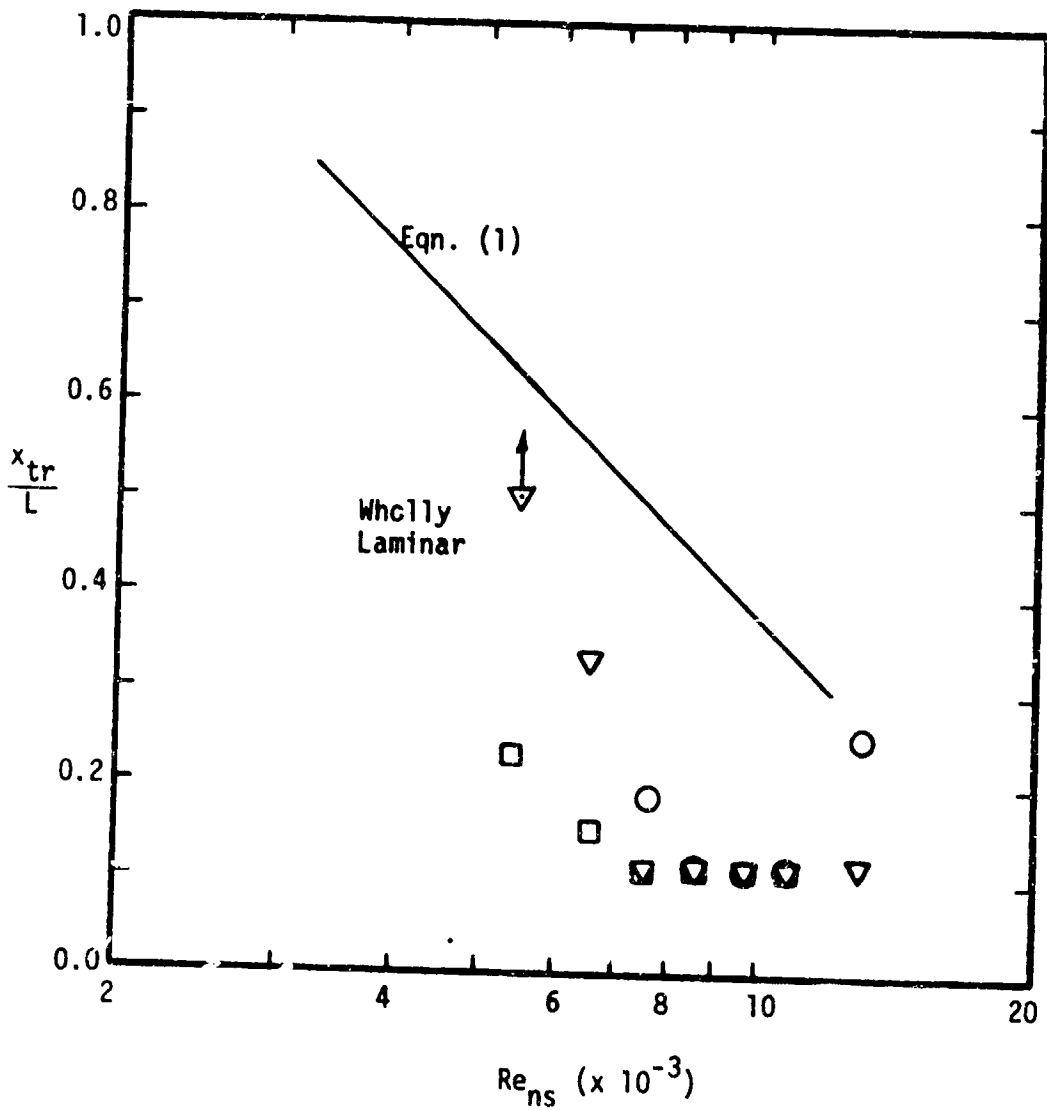
Figure 8. - The transition location as a function of Re_{ns} for C7 with $k = 0.0254$ cm (0.010 in.)
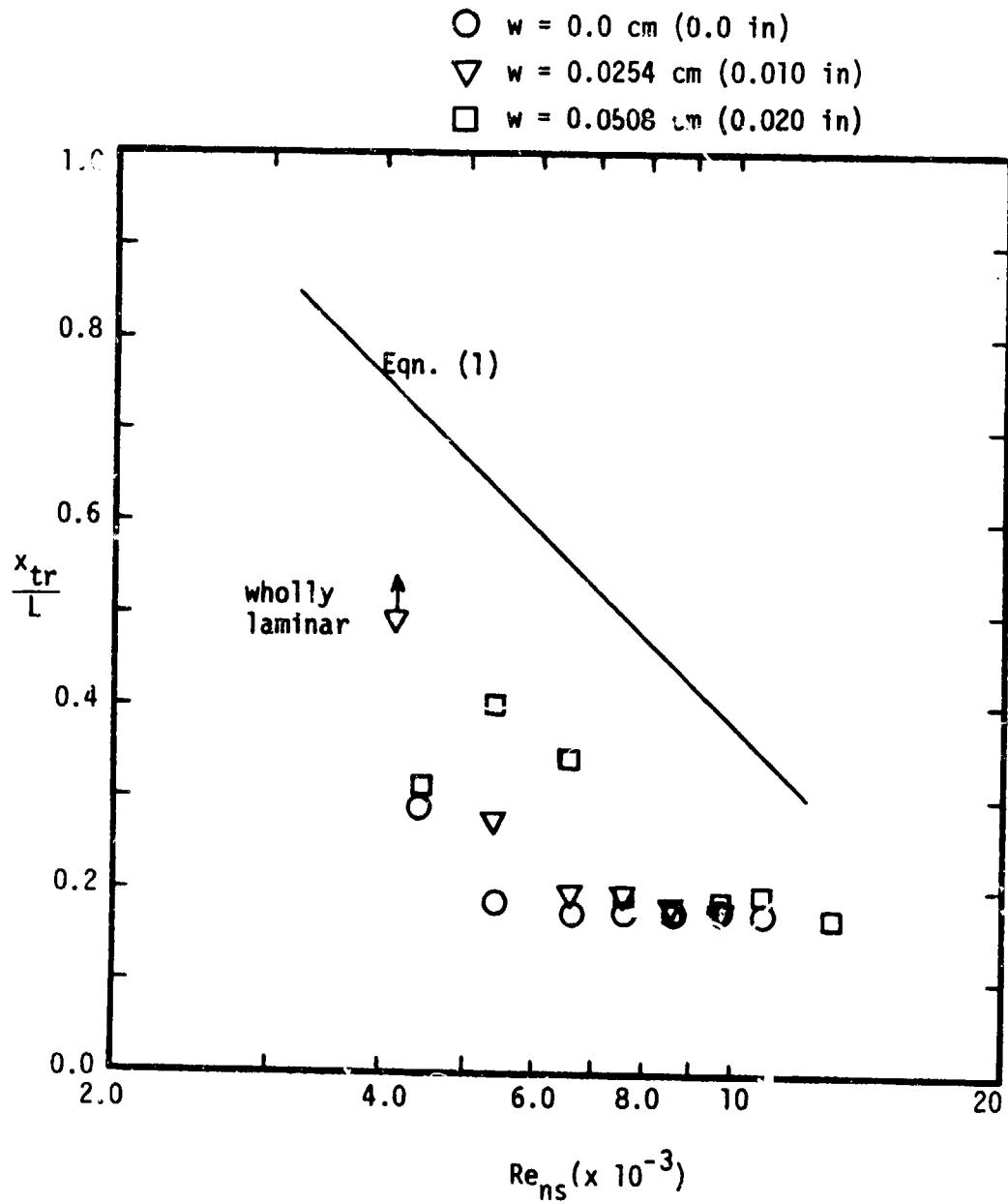
Figure 9. - A correlation of the transition locations for C8 with k = 0.0381 cm (0.015 in).
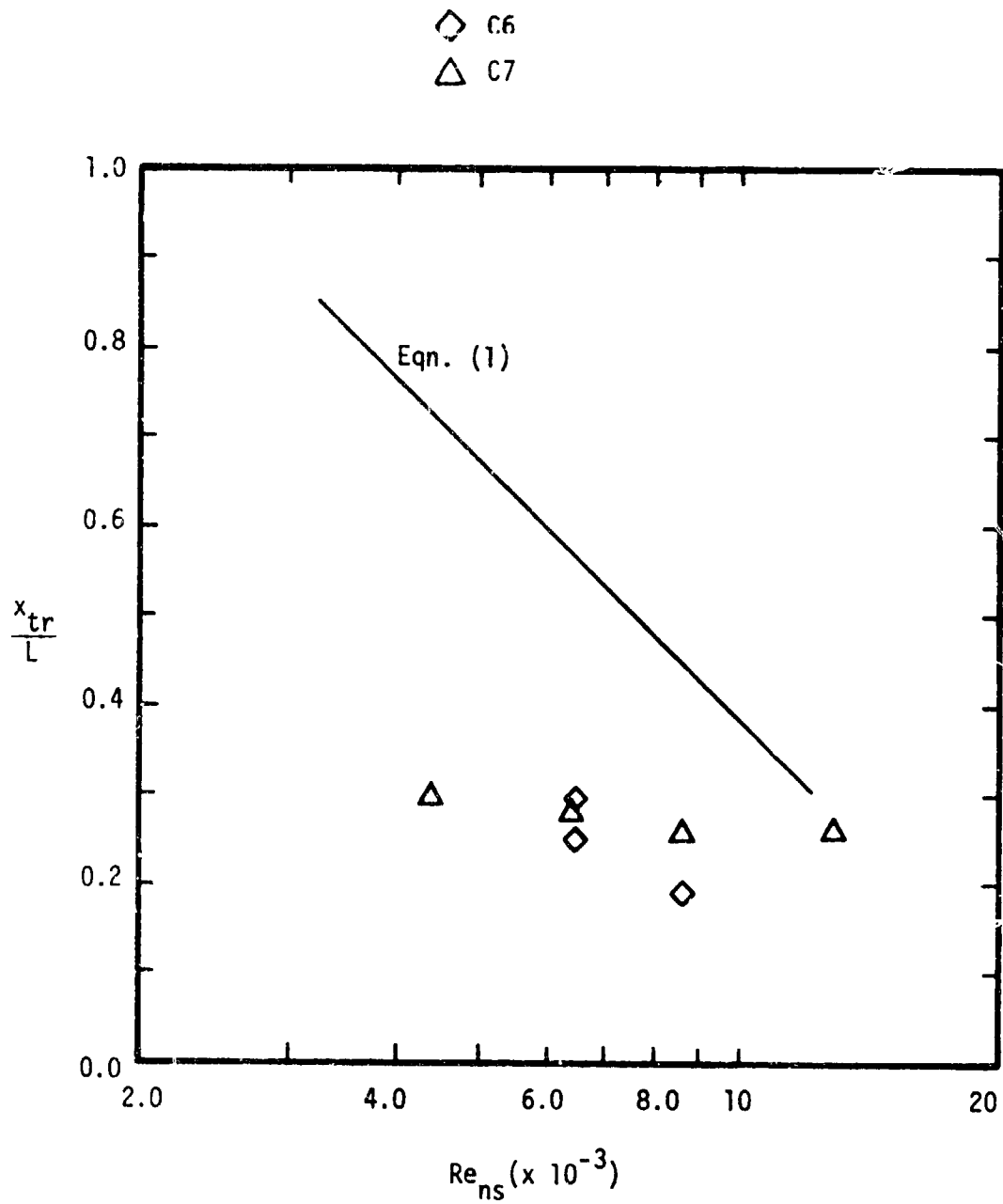
Figure 10. - A correlation of the transition locations showing the effect of gap-only roughness, w = 0.0254 cm (0.010 in), k = 0.0 cm (0.0 in).
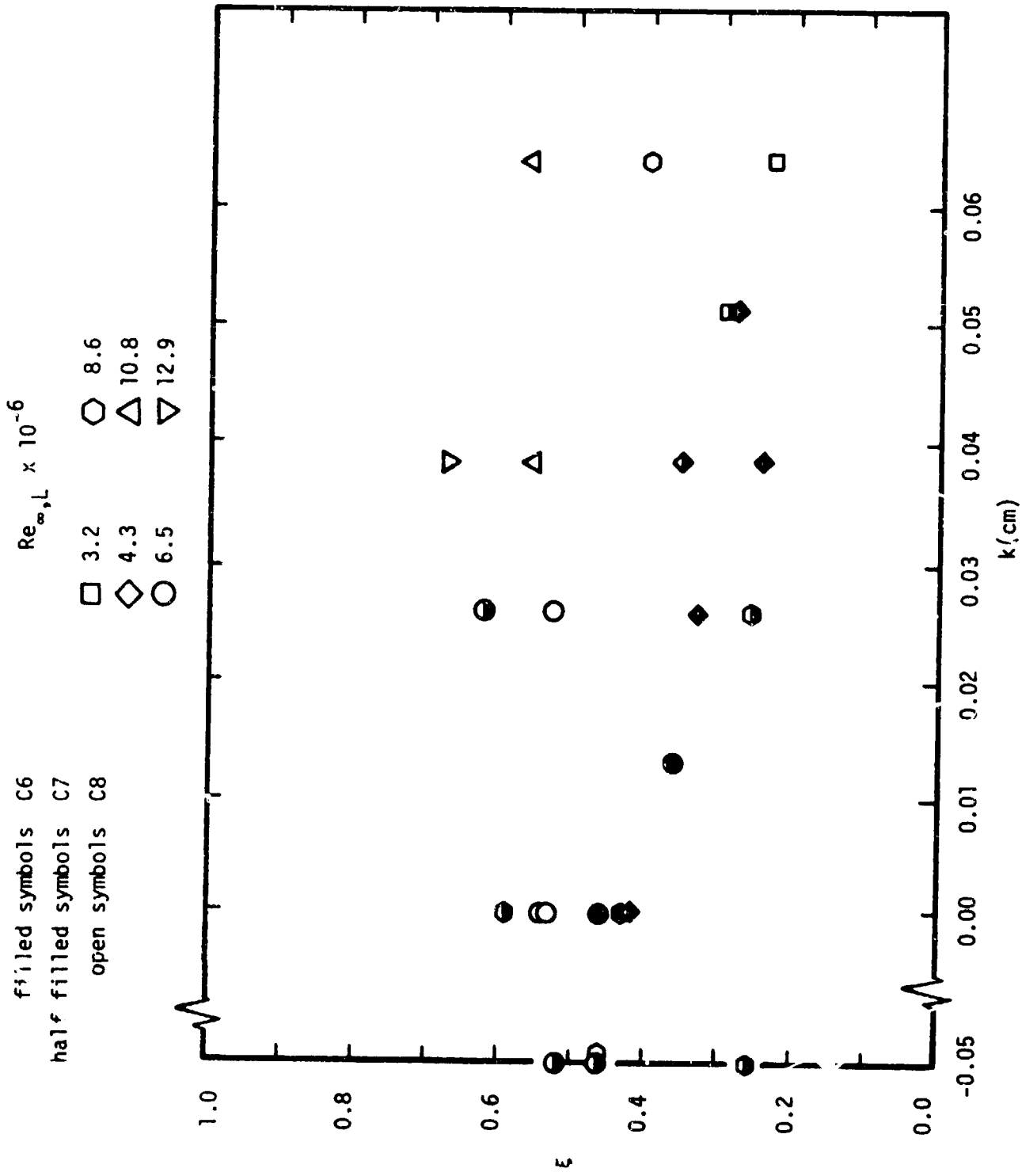
Figure 11. - The relative transition location as a function of tile height for $w = 0.0254$ cm (0.010 in.)

Data from Ref. 14.

Data from the current test program

$Re_{\infty,L} \times 10^{-6}$

◇ 4.3   ◇ 5.3   ♂ 7.5   ⬡ 8.6

filled symbols: C6
half filled symbols: C7
open symbols: C8

ε
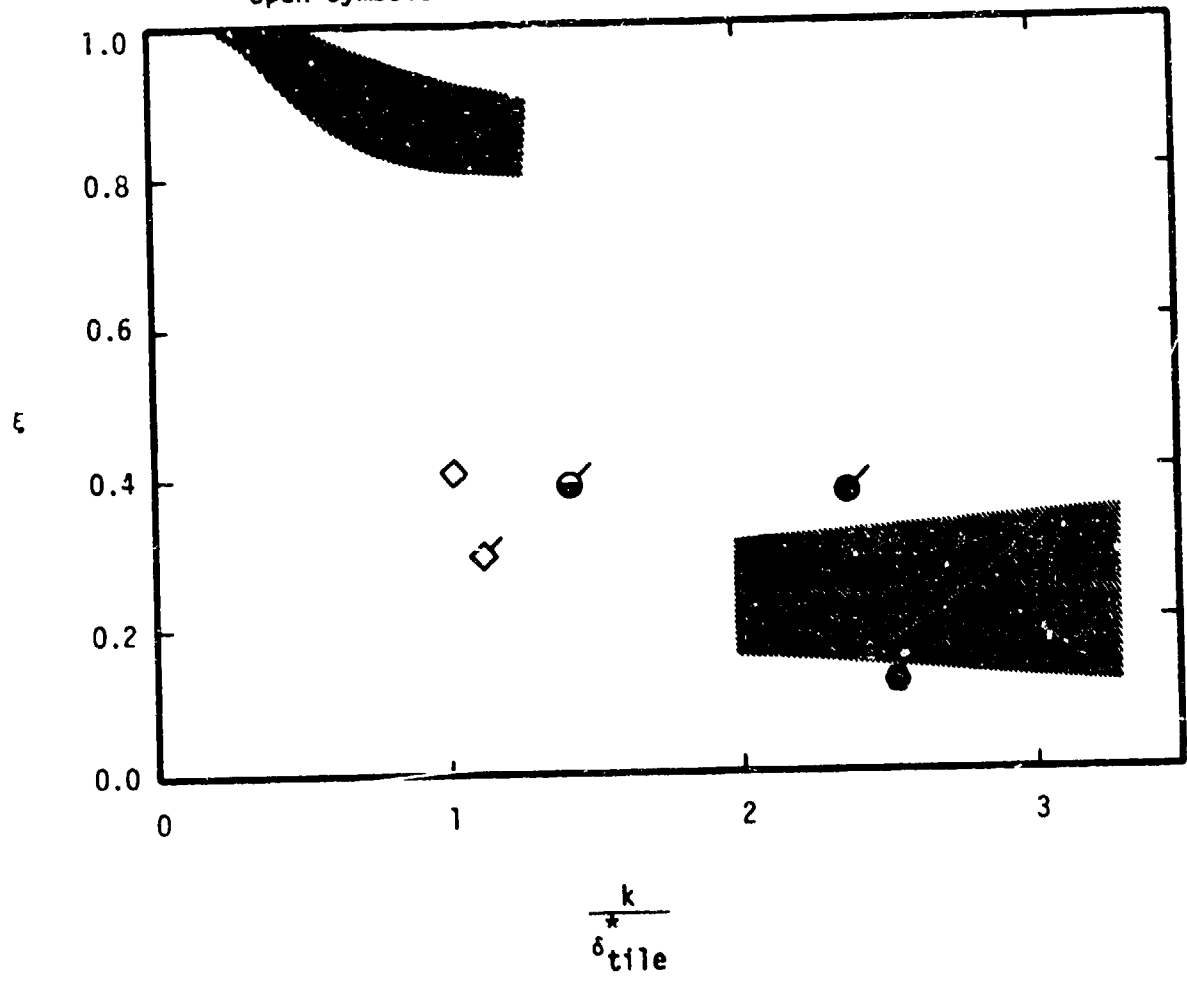
$\dfrac{k}{\delta^*_{tile}}$

Figure 12. - The relative transition location as a function k/δ^*_{tile}
for configurations where w = 0.00 cm (0.00 in.)
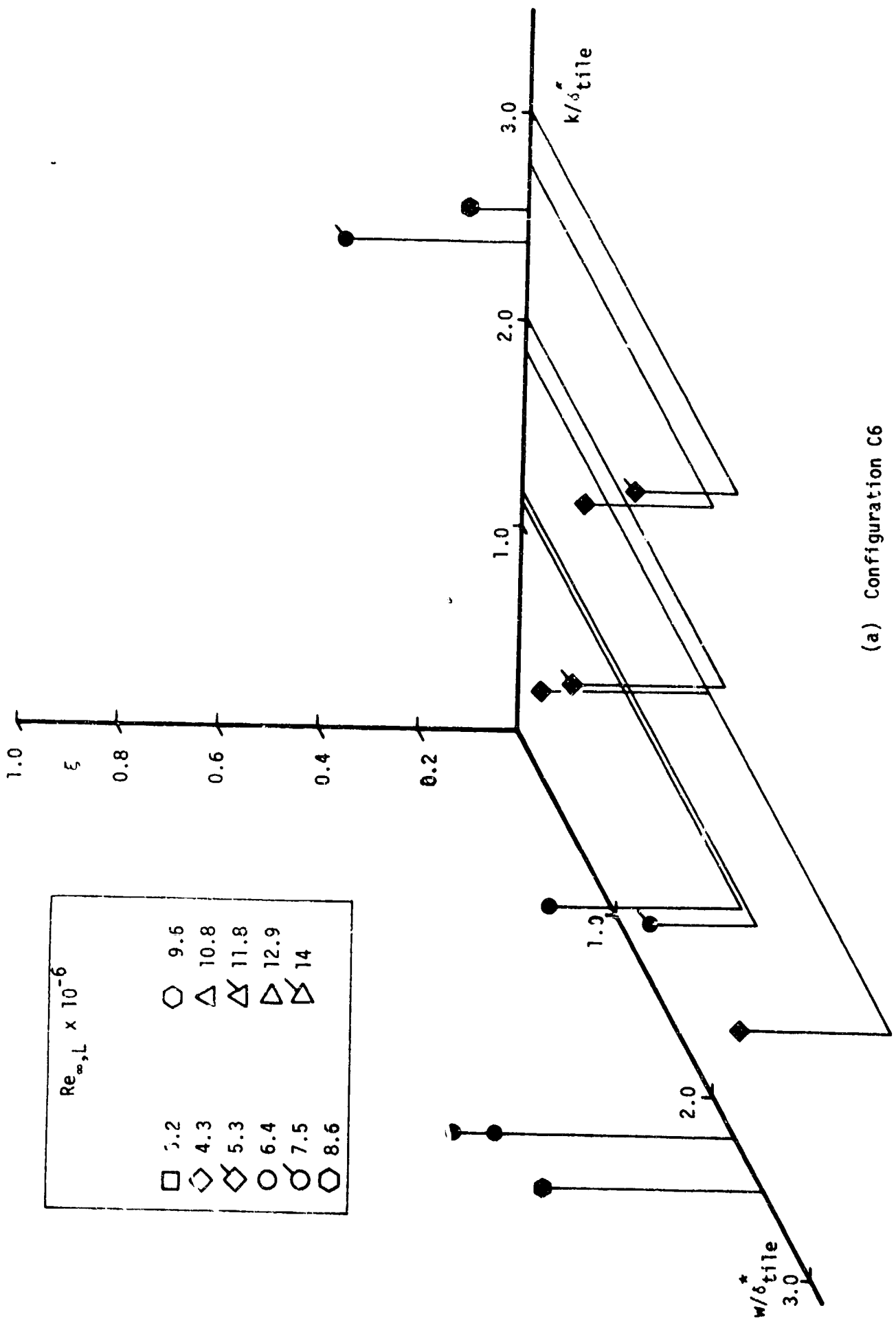
(a) Configuration C6

Figure 13. – The relative transition locations as a function both of w/δ^*_{tile} and k/δ^*_{tile}
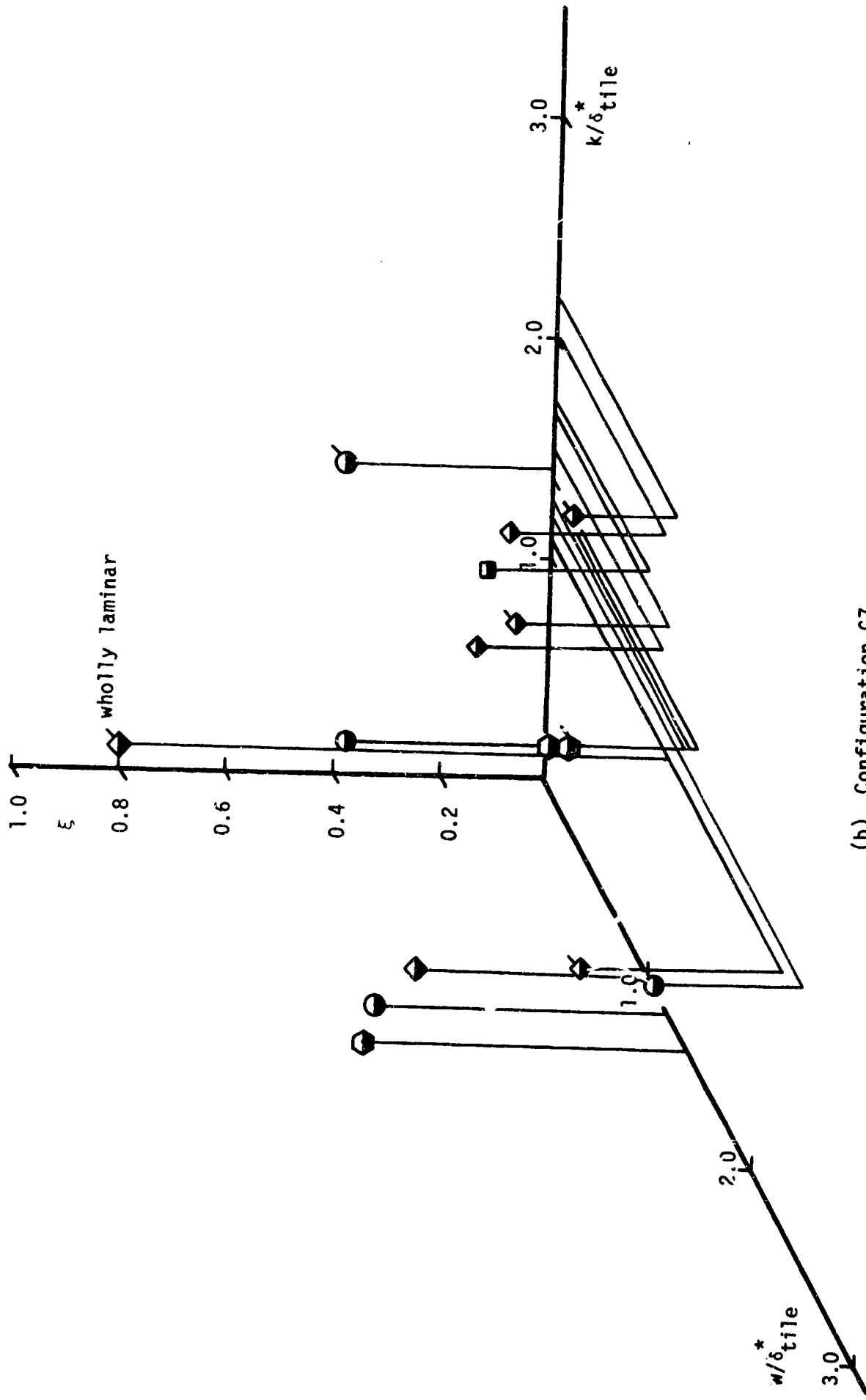
(b) Configuration C7

Figure 13. - Continued
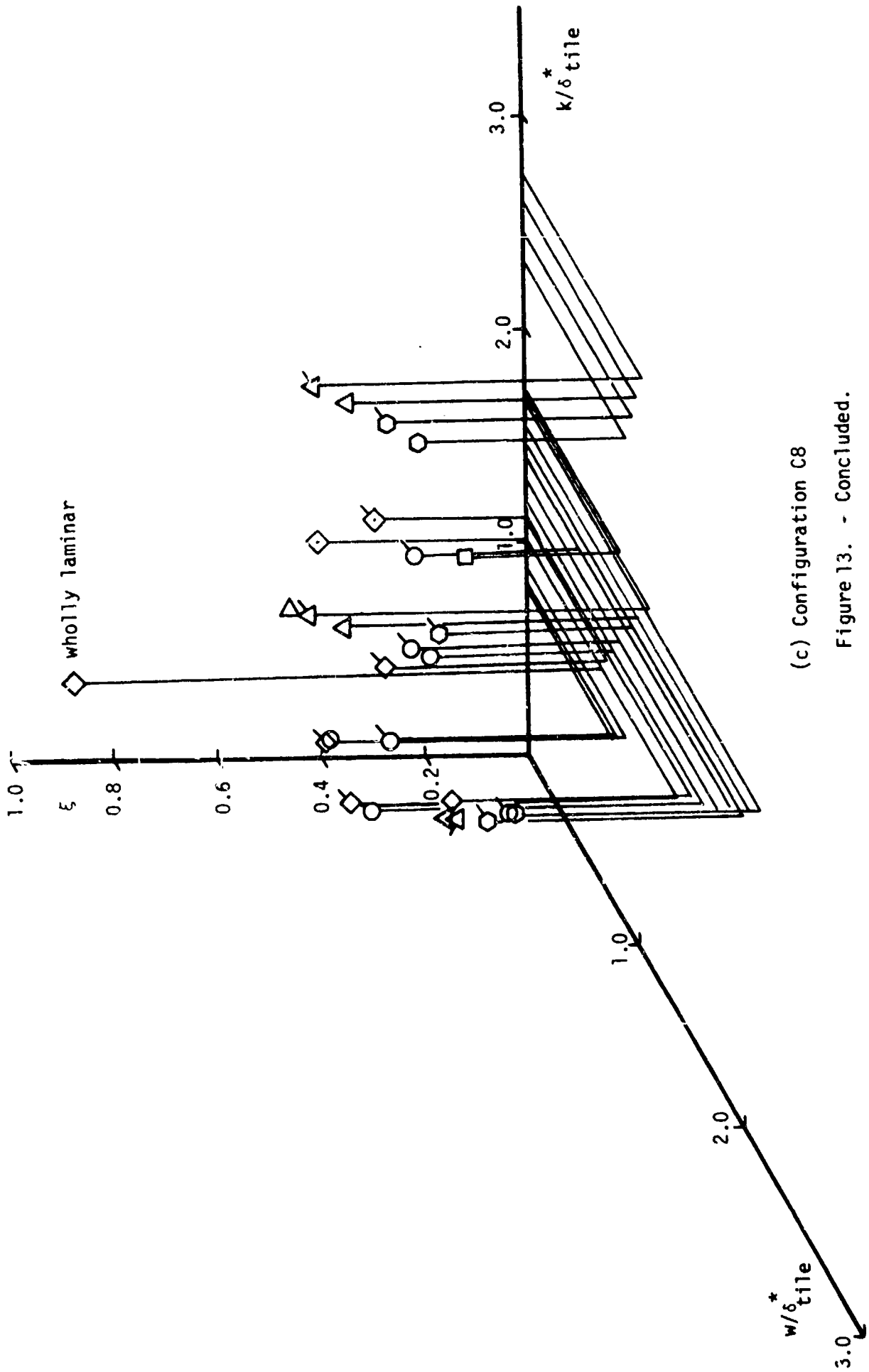
(c) Configuration C8

Figure 13. - Concluded.
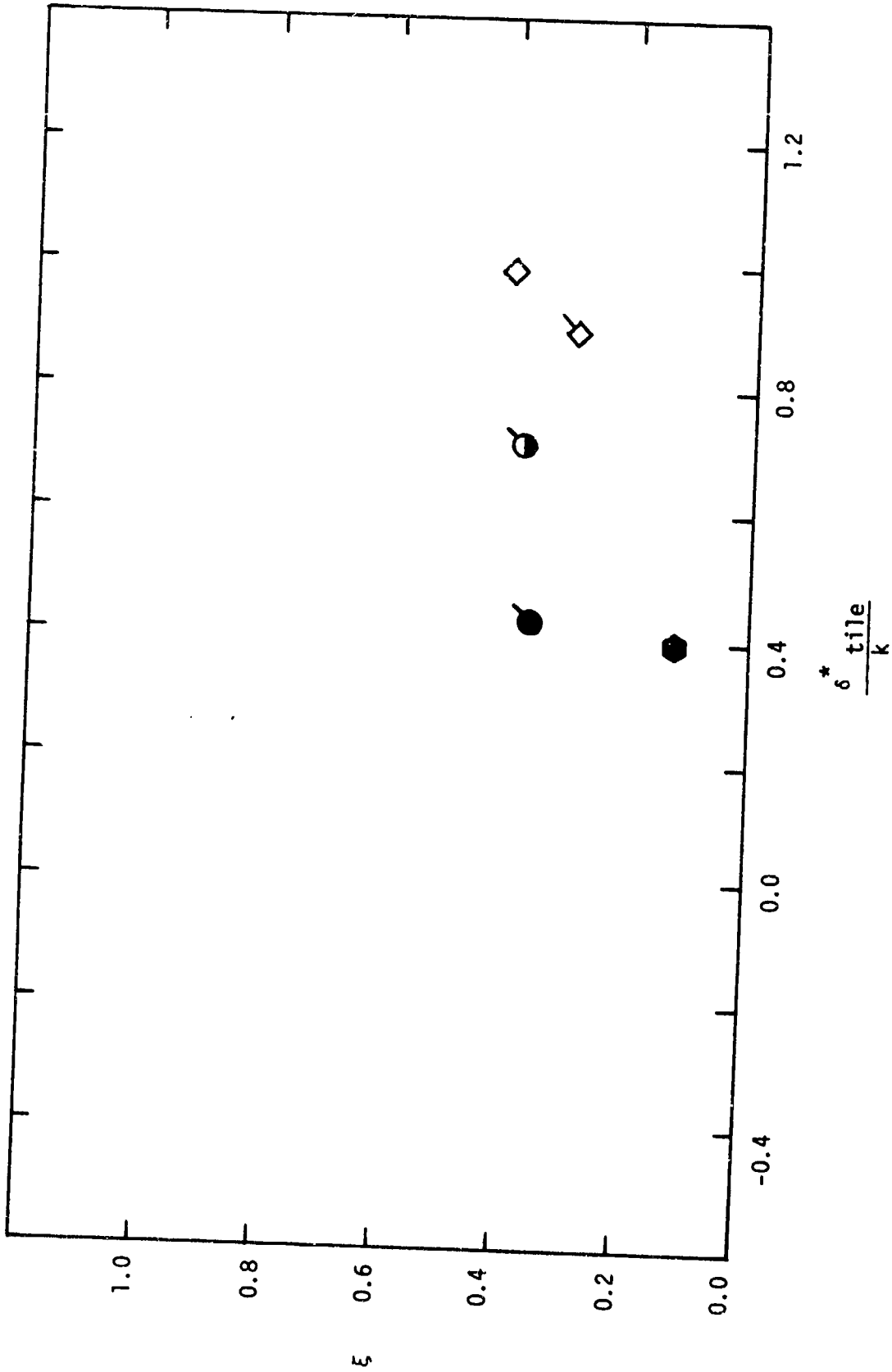
(a)   w = 0.0 cm (0.000 in.)

Figure 14. - The relative transition location as a function of $\dfrac{\delta^*_{tile}}{k}$
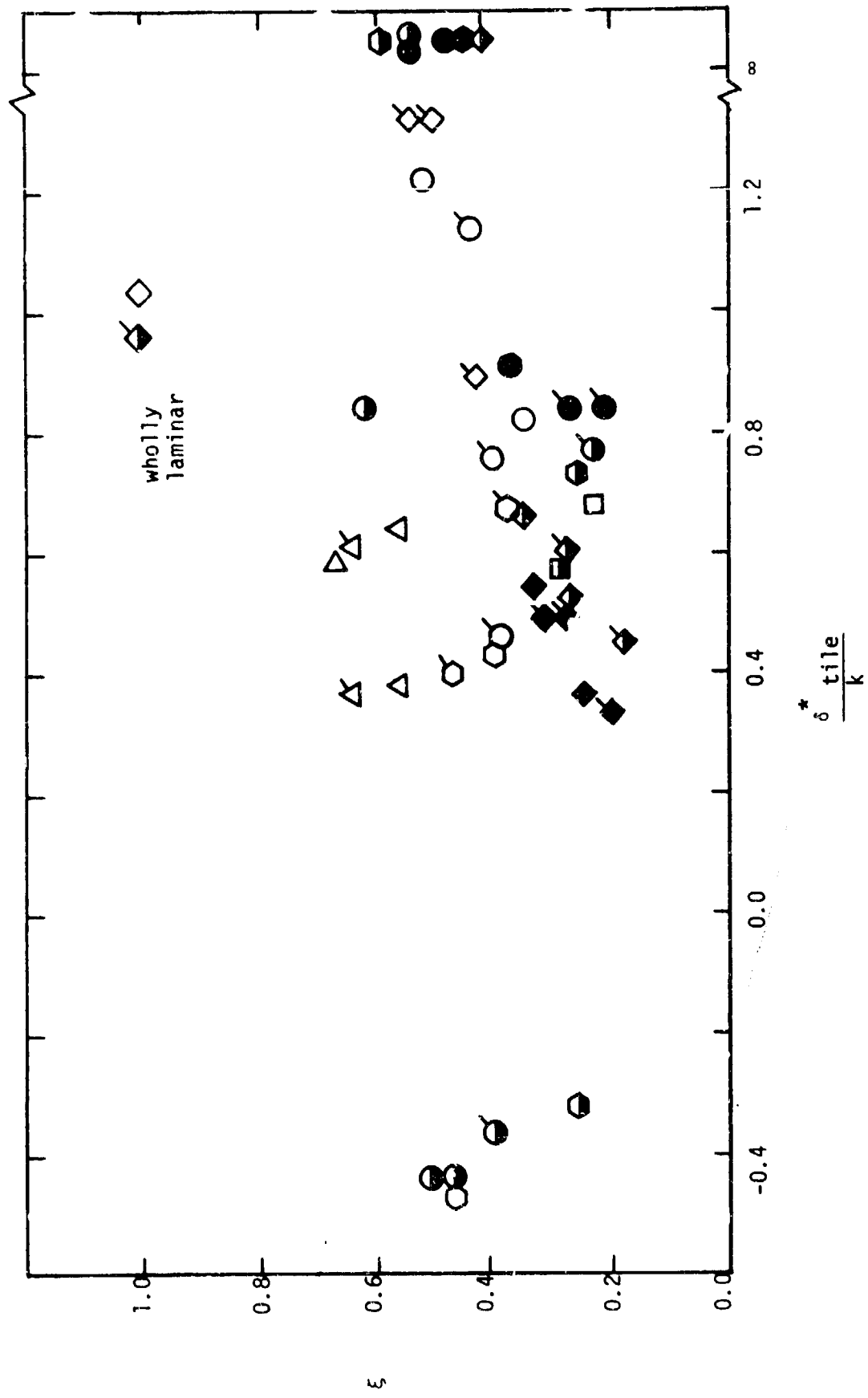
(b) $w = 0.0254$ cm (0.010 in)

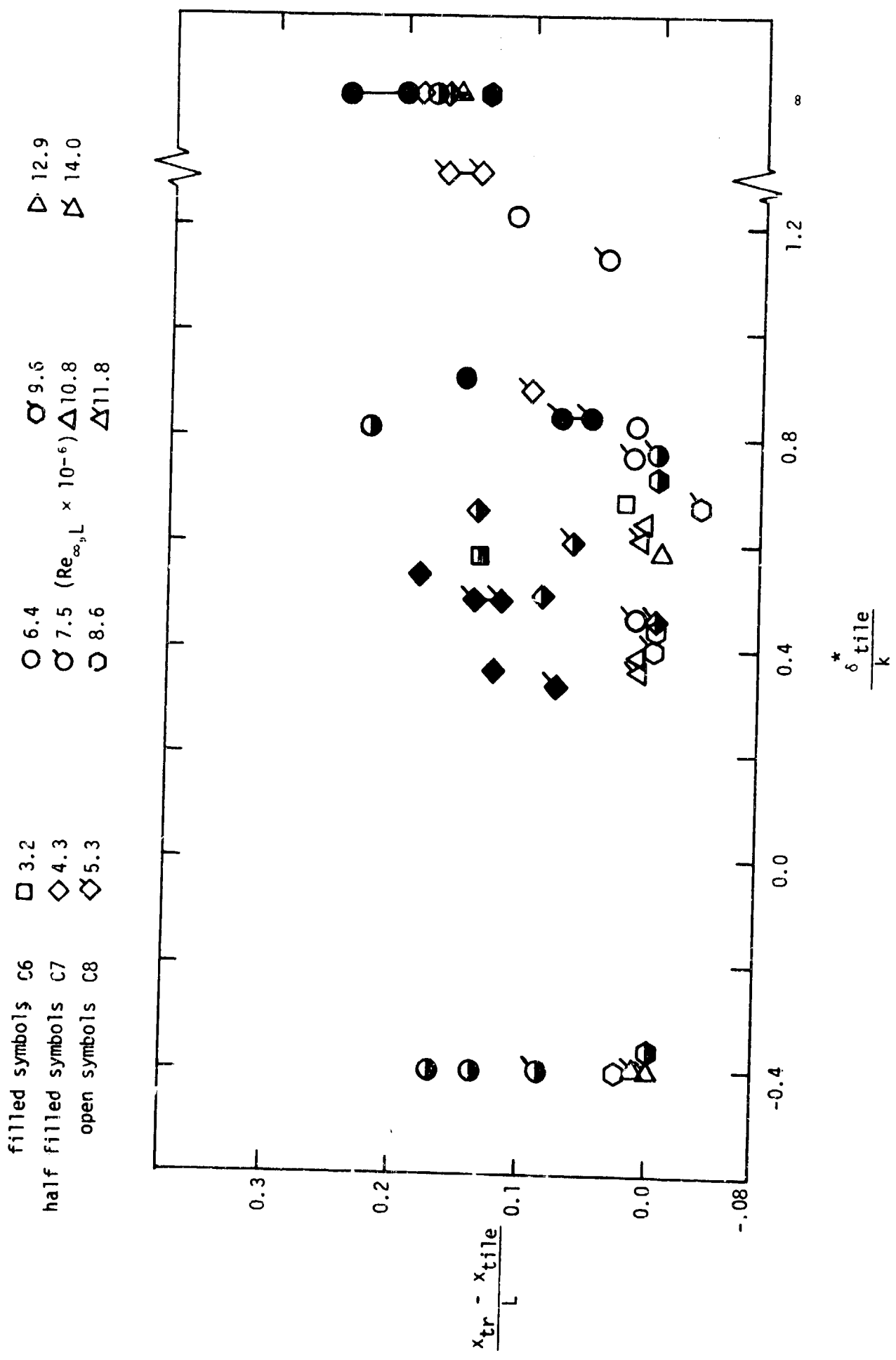Figure 14. – Continued
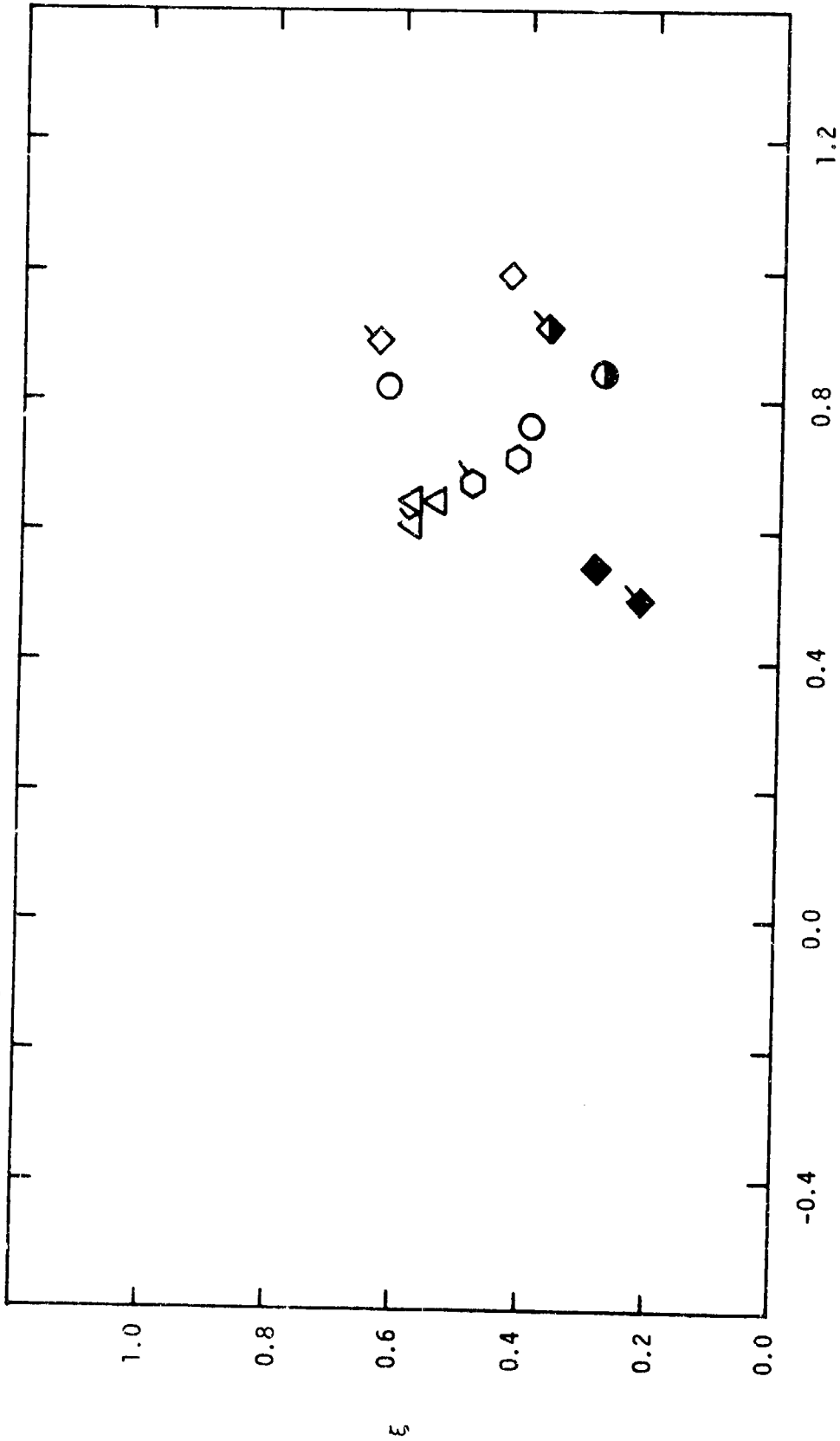
(c) w = 0.0508 cm (0.020 in)

Figure 14. - Concluded.

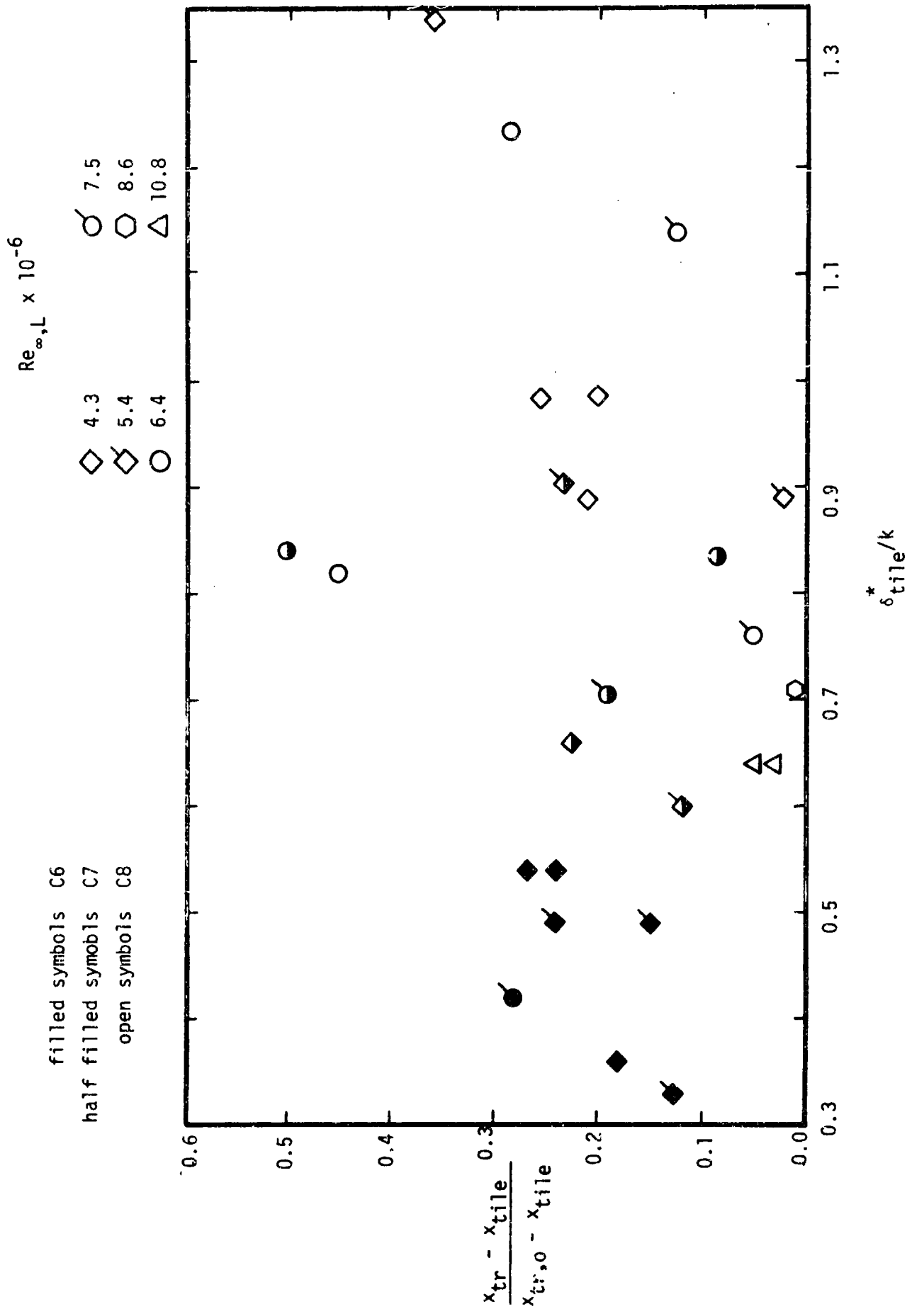Figure 15. - The distance from the tiles to the transition location as a function of δ^*_{tile}/k.

Figure 16. – Selected data for the relative transition location in terms of the distance from the tiles to the transition location for various gap width
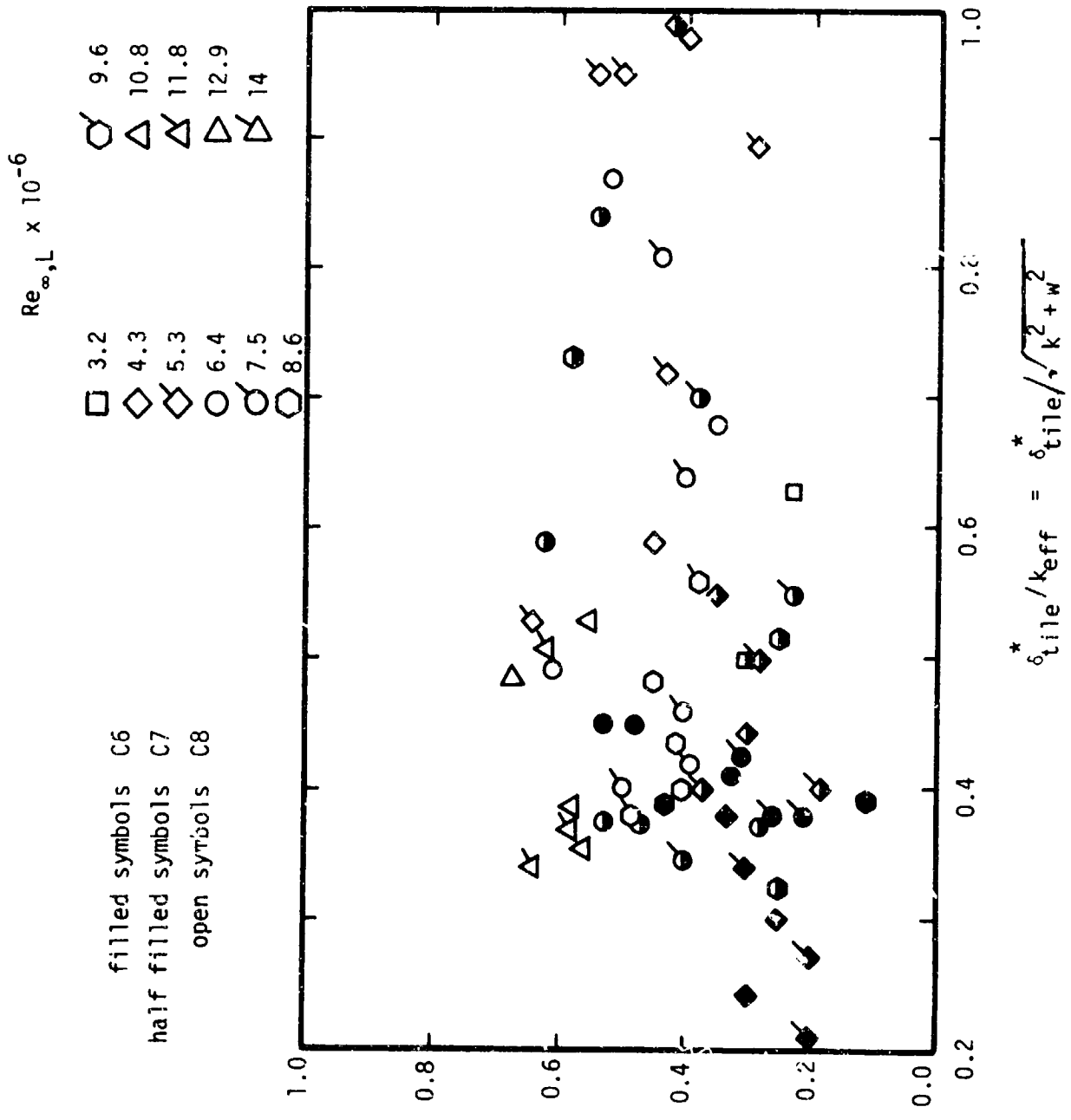
$Re_{\infty,L} \times 10^{-6}$

□	3.2	◇	9.6
◇	4.3	△	10.8
◇	5.3	△	11.8
○	6.4	△	12.9
○	7.5	△	14
⬡	8.6		

$$\delta^*_{tile}/k_{eff} = \frac{\delta^*_{tile}}{\sqrt{k^2 + w^2}}$$

ε

Figure 17. – The relative transition location as a function of δ^*_{tile}/k_{eff} .